1521-0111/88/2/401–420$25.00
MOLECULAR PHARMACOLOGY

http://dx.doi.org/10.1124/mol.115.099291
Mol Pharmacol 88:401–420, August 2015

A Multifaceted $GABA_A$ Receptor Modulator: Functional Properties and Mechanism of Action of the Sedative-Hypnotic and Recreational Drug Methaqualone (Quaalude)

Harriet Hammer, Benjamin M. Bader, Corina Ehnert, Christoffer Bundgaard, Lennart Bunch, Kirsten Hoestgaard-Jensen, Olaf H.-U. Schroeder, Jesper F. Bastlund, Alexandra Gramowski-Voß, and Anders A. Jensen

Department of Drug Design and Pharmacology, Faculty of Health and Medical Sciences, University of Copenhagen, Copenhagen, Denmark (H.H., L.B., K.H.-J., A.A.J.); NeuroProof, Rostock, Germany (B.M.B., C.E., O.H.-U.S., A.G.-V.); and H. Lundbeck A/S, Valby, Denmark (C.B., J.F.B.)

Received March 29, 2015; accepted June 8, 2015

ABSTRACT

In the present study, we have elucidated the functional characteristics and mechanism of action of methaqualone (2-methyl-3-o-tolyl-4(3*H*)-quinazolinone, Quaalude), an infamous sedative-hypnotic and recreational drug from the 1960s–1970s. Methaqualone was demonstrated to be a positive allosteric modulator at human $\alpha_{1,2,3,5}\beta_{2,3}\gamma_{2S}$ $GABA_A$ receptors ($GABA_A$Rs) expressed in *Xenopus* oocytes, whereas it displayed highly diverse functionalities at the $\alpha_{4,6}\beta_{1,2,3}\delta$ $GABA_A$R subtypes, ranging from inactivity ($\alpha_4\beta_1\delta$), through negative ($\alpha_6\beta_1\delta$) or positive allosteric modulation ($\alpha_4\beta_2\delta$, $\alpha_6\beta_{2,3}\delta$), to superagonism ($\alpha_4\beta_3\delta$). Methaqualone did not interact with the benzodiazepine, barbiturate, or neurosteroid binding sites in the $GABA_A$R. Instead, the compound is proposed to act through the transmembrane $\beta^{(+)}/\alpha^{(-)}$ subunit interface of the receptor, possibly targeting a site overlapping with that of the general anesthetic etomidate. The negligible activities displayed by methaqualone at numerous neurotransmitter receptors and transporters in an elaborate screening for additional putative central nervous system (CNS) targets suggest that it is a selective $GABA_A$R modulator. The mode of action of methaqualone was further investigated in multichannel recordings from primary frontal cortex networks, where the overall activity changes induced by the compound at 1–100 μM concentrations were quite similar to those mediated by other CNS depressants. Finally, the free methaqualone concentrations in the mouse brain arising from doses producing significant in vivo effects in assays for locomotion and anticonvulsant activity correlated fairly well with its potencies as a modulator at the recombinant $GABA_A$Rs. Hence, we propose that the multifaceted functional properties exhibited by methaqualone at $GABA_A$Rs give rise to its effects as a therapeutic and recreational drug.

Introduction

Methaqualone (2-methyl-3-o-tolyl-4(3*H*)-quinazolinone) has a colorful history as a therapeutic and recreational drug. Methaqualone was marketed in the early 1960s as a nonbarbiturate hypnotic with a wide safety margin and low abuse potential under trade names like Quaalude, Parest, Somnafac, Revonal, and as the combination drug Mandrax (with the antihistamine diphenhydramine). In the subsequent years, methaqualone became one of the best-selling sedative-hypnotic drugs worldwide, with several structural analogs following in its trail (collectively referred to as "quaaludes") (Carroll and Gallo, 1985; Gass, 2008). However, clinical use of the drug soon revealed that besides giving rise to serious adverse effects, it was highly addictive and induced tolerance and cross-tolerance with other hypnotics. Moreover, concomitantly with its therapeutic use, methaqualone became highly popular as a recreational drug, where it often was consumed in combination with alcohol (known as "luding out") (Falco, 1976; McCarthy et al., 2005; Gass, 2008; Herzberg, 2011). These problems led to the implementation of tighter regulation of the drug, and by the mid-1980s, it had been withdrawn from most markets (Carroll and Gallo, 1985; Gass, 2008). Nevertheless, recreational use of illegally produced methaqualone still constitutes a substantial health problem in some parts of the world (Parry et al., 2004; McCarthy et al., 2005).

The overall clinical properties of methaqualone are very characteristic for a sedative-hypnotic drug; however, some of its in vivo effects differ from those induced by classic central nervous system (CNS) depressants. Methaqualone reportedly

This study was supported financially by the Novo Nordisk Foundation. The in vitro binding profiling of methaqualone was generously provided by the National Institute of Mental Health's Psychoactive Drug Screening Program (NIMH PDSP) [Grant HHSN-271-2008-025C]. The NIMH PDSP is directed by Bryan L. Roth at the University of North Carolina at Chapel Hill and project officer Jamie Driscol at NIMH, Bethesda, MD.
dx.doi.org/10.1124/mol.115.099291.

ABBREVIATIONS: CNS, central nervous system; DS2, 4-chloro-*N*-[2-(2-thienyl)imidazo[1,2-*a*]pyridine-3-yl benzamide; $GABA_A$Rs, GABA type A receptors; MEA, microelectrode array; MEST, maximal electroshock seizures threshold; MK801, (5*S*,10*R*)-(+)-5-methyl-10,11-dihydro-5*H*-dibenzo[*a*,*d*]cyclohepten-5,10-imine maleate, NAM, negative allosteric modulator; PAM, positive allosteric modulator; PDSP, Psychoactive Drug Screening Program; TEVC, two-electrode voltage clamp; WT, wild-type.

mediates a rapid induction of a more natural deep sleep that results in less severe dizziness/dullness and headaches in insomnia patients than benzodiazepines and barbiturates (Barcelo, 1961; Ionescu-Pioggia et al., 1988). Furthermore, unlike most sedatives, methaqualone is also quite efficacious as an antispasmodic (Gass, 2008). Finally, the euphoria and aphrodisiac properties constituting some of the major psychologic effects evoked by methaqualone in its recreational use are effects not typically associated with CNS depressants (Falco, 1976; Ionescu-Pioggia et al., 1988; Gass, 2008; Barceloux, 2012). Although the electroencephalographic effects induced by methaqualone in rodent and human brains largely resemble those produced by barbiturates and other CNS depressants, the fact that some qualitative differences have been observed between these drugs in these recordings seems to support the clinical observations (Pfeiffer et al., 1968; Saxena et al., 1977).

Whereas the therapeutic and psychotropic effects of methaqualone arguably have been comprehensively documented, the molecular basis for these effects has never been investigated. Based on the overall similarities between its behavioral effects and those induced by barbiturates and benzodiazepines, methaqualone has been assumed to act through the GABA type A receptors ($GABA_A$Rs) (Carroll and Gallo, 1985; Gass, 2008). This family of ligand-gated anion channels comprises a plethora of receptors assembled from 19 subunits ($\alpha_{1–6}$, $\beta_{1–3}$, $\gamma_{1–3}$, δ, ε, θ, π, and $\rho_{1–3}$), and the complexity of GABAergic neurotransmission largely arises from differential regional and cellular expression of these subtypes (Whiting, 2003; Olsen and Sieghart, 2008; Brickley and Mody, 2012). The pentameric $GABA_AR$ complex is typically composed of two α subunits, two β subunits, and a γ or δ subunit; and the receptor comprises numerous allosteric sites through which GABA-evoked signaling can be modulated by various drugs, including barbiturates, benzodiazepines, neurosteroids, and anesthetics (Sieghart, 2015). In contrast to the well established role of $GABA_A$Rs as the principal mediators of the effects of these drugs, however, the link between methaqualone and GABAergic neurotransmission is founded on strikingly sparse and largely inconclusive experimental data (Müller et al., 1978; Naik et al., 1978; Hicks et al., 1990).

In the present study, methaqualone has been subjected to an elaborate functional characterization at human $GABA_AR$ subtypes expressed in *Xenopus* oocytes, and its molecular mechanism of action at the receptors has been delineated. Furthermore, the functionality of methaqualone at native $GABA_A$Rs has been elucidated by multiparametric analysis of its electrophysiologic effects at cortical neuron network activity. Finally, the correlation between the functional properties of methaqualone at $GABA_A$Rs in vitro and its in vivo efficacy in mice models for locomotion and anticonvulsant activity has been investigated.

Materials and Methods

GABA, diazepam, $ZnCl_2$, and chemicals for buffers were obtained from Sigma-Aldrich (St. Louis, MO). Methaqualone (Fig. 1A) was synthesized by the MedChem Department at H. Lundbeck A/S. Pentobarbital and allopregnanolone were purchased from May and Baker (Dagenham, UK) and Merck Chemicals (Nottingham, UK), respectively. Flumazenil and etomidate were purchased from Abcam Biochemicals (Cambridge, UK), and DS2 (4-chloro-*N*-[2-(2-thienyl)imidazo[1,2-*a*]pyridine-3-yl benzamide) was obtained from Tocris Cookson (Bristol, UK). Defolliculated stage V or VI oocytes harvested from female *Xenopus laevis* frogs (using MS222 as anesthetic) were obtained from Lohmann Research Equipment (Castrop-Rauxel, Germany).

Molecular Biology

The subcloning of human α_1-α_6, β_1, β_2, δ, and γ_{2S} cDNAs into pcDNA3.1 has been described previously (Jensen et al., 2010; Hoestgaard-Jensen et al., 2014), and the human β_3 cDNA used in this study was in pGEMHE. Point mutations were introduced into cDNAs using the QuikChange mutagenesis kit (Stratagene, Santa Clara, CA) and oligonucleotides from TAG Copenhagen A/S (Copenhagen, Denmark). The integrity and the absence of unwanted mutations in all cDNAs created by polymerase chain reaction were verified by DNA sequencing (Eurofins MWG Operon, Ebersberg, Germany).

Xenopus laevis Oocytes and Two-Electrode Voltage Clamp Recordings

The functional characterization of methaqualone at wild-type (WT) and mutant $GABA_A$Rs expressed in *Xenopus* oocytes was performed essentially as previously described (Hoestgaard-Jensen et al., 2013). The $GABA_AR$ cDNAs were linearized and applied as templates for in vitro cRNA synthesis using the T7 mMESSAGE mMACHINE High Yield Capped RNA transcription kit (Life Technologies Corp., Carlsbad, CA. Either 9 or 18 nl cRNA encoding for $\alpha_1\beta_2$ (α_1:β_2 ratio: 0.06:0.06 μg/μl) and $\alpha_{1,2,3,5}\beta_{2,3}\gamma_{2S}$ $GABA_A$Rs (α:β:γ_{2S} ratio: 0.01:0.01:0.01 μg/μl), or 46 nl cRNA encoding for $\alpha_6\beta_2$ (α_6:β_2 ratio: 1:0.1 μg/μl) and $\alpha_{4,6}\beta_{1,2,3}\delta$ $GABA_A$Rs (α:β:δ ratio: 1:0.1:1 μg/μl) were injected into oocytes, which subsequently were incubated at 18°C in modified Barth's solution [88 mM NaCl, 1 mM KCl, 15 mM HEPES (pH 7.5), 2.4 mM $NaHCO_3$, 0.41 mM $CaCl_2$, 0.82 mM $MgSO_4$, 0.3 mM $Ca(NO_3)_2$, 100 U/ml penicillin and 100 μg/ml streptomycin]. Whole-cell currents in the $\alpha_1\beta_2/\alpha_{1,2,3,5}\beta_{2,3}\gamma_{2S}$- and $\alpha_6\beta_2/\alpha_{4,6}\beta_{1,2,3}\delta$-expressing oocytes were measured 1–4 and 3–6 days after cRNA injection, respectively. In the two-electrode voltage-clamp (TEVC) recordings, the oocytes were placed in a recording chamber continuously perfused with a saline solution [115 mM NaCl, 2.5 mM KCl, 10 mM HEPES (pH 7.5), 1.8 mM $CaCl_2$, 0.1 mM $MgCl_2$], and the test compounds were applied in the perfusate. Both voltage and current electrodes were agar-plugged with 3 M KCl and displayed resistances between 0.5–2.0 MΩ. Oocytes were voltage-clamped at −40 mV to −80 mV (depending on the current size) using an Oocyte Clamp OC-725C amplifier (Warner Instruments, Hamden, CT). The incorporation of the γ_{2S} subunit into the $GABA_A$Rs assembled at the cell surface of $\alpha_{1,2,3,5}\beta_{2,3}\gamma_{2S}$-expressing oocytes was confirmed on a routine basis with 100 μM $ZnCl_2$ (Karim et al., 2013), and the presence of δ in cell surface-expressed receptors in $\alpha_{4,6}\beta_{1,2,3}\delta$-injected oocytes was verified using the δ-$GABA_AR$ selective positive allosteric modulator (PAM) DS2 (1 μM) and 1 μM $ZnCl_2$ (Storustovu and Ebert, 2006; Wafford et al., 2009; Karim et al., 2012).

In the experiments where the functional properties of GABA or methaqualone as agonists at the various receptors were characterized, 10 μM GABA was applied to the perfusate until the peak of the response was observed, usually within 30 seconds. When two consecutive applications of GABA had elicited responses of comparable sizes (±5%), various concentrations of GABA or methaqualone were applied. In the experiments where the functional properties of various allosteric modulators were characterized, the GABA concentration to be used (GABA EC_{10} or GABA $EC_{60–70}$) was determined on the day of the experiment by measurements on two oocytes expressing the specific receptor. Subsequently, when two consecutive applications of GABA EC_{10} or GABA $EC_{60–70}$ were applied to the perfusate and observed to elicit currents of comparable sizes (±5%), the functional characteristics of the allosteric modulators at the $GABA_AR$

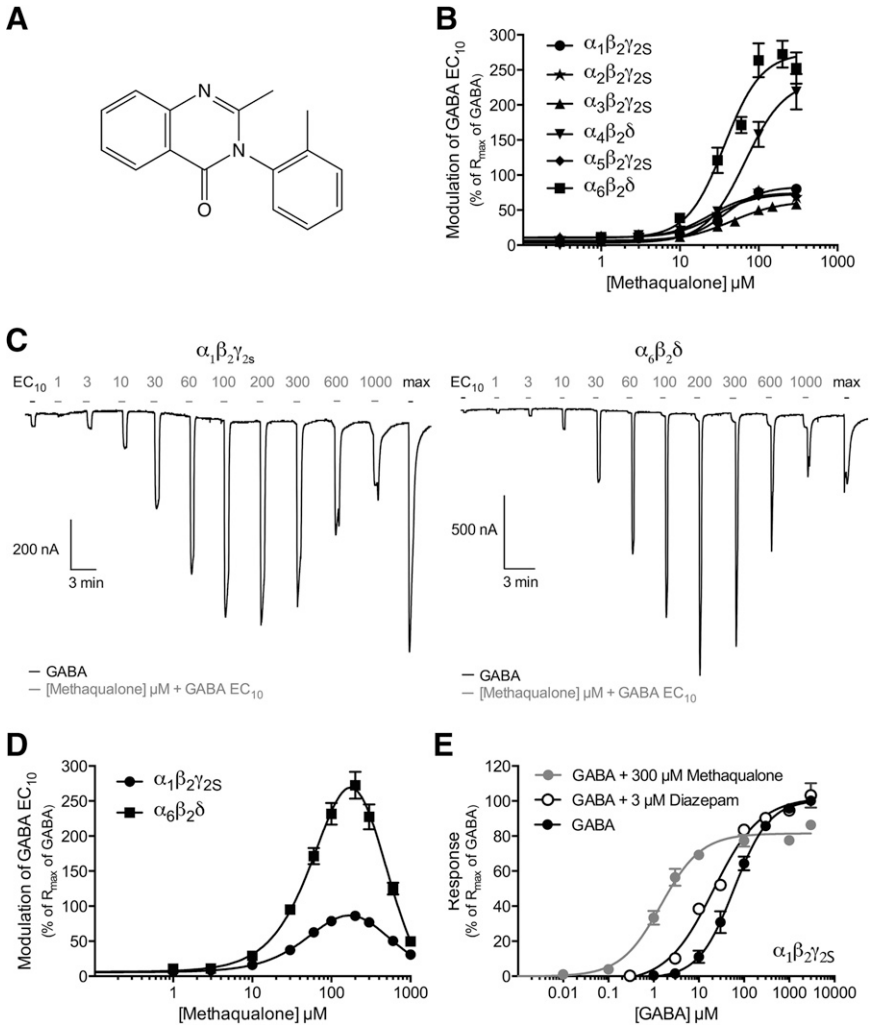

Fig. 1. Functional properties of methaqualone at human $GABA_AR$s expressed in *Xenopus* oocytes. (A) Chemical structure of methaqualone. (B) Concentration-response curves for methaqualone at $\alpha_1\beta_2\gamma_{2S}$, $\alpha_2\beta_2\gamma_{2S}$, $\alpha_3\beta_2\gamma_{2S}$, $\alpha_4\beta_2\delta$, $\alpha_5\beta_2\gamma_{2S}$, and $\alpha_6\beta_2\delta$ $GABA_AR$s in the presence of GABA EC_{10} (means ± S.E.M.; n = 5–9). (C) Representative traces for various concentrations of methaqualone coapplied with GABA EC_{10} at $\alpha_1\beta_2\gamma_{2S}$ (left) and $\alpha_6\beta_2\delta$ (right) $GABA_AR$s. The application bars in gray for the various methaqualone concentrations all represent a 30-second preincubation with methaqualone followed by coapplication of methaqualone and GABA EC_{10}. The black application bars represent application of GABA EC_{10} and the GABA concentration eliciting the maximal response. (D) Concentration-response curves for methaqualone at $\alpha_1\beta_2\gamma_{2S}$ and $\alpha_6\beta_2\delta$ $GABA_AR$s in the presence of GABA EC_{10} (means ± S.E.M.; n = 5–6). (E) Concentration-response curves for GABA at the $\alpha_1\beta_2\gamma_{2S}$ $GABA_AR$ in the absence or presence of 3 μM diazepam or 300 μM methaqualone (means ± S.E.M.; n = 4–6).

were determined by preapplication of the modulator to the perfusate 30 seconds before coapplication of the modulator and GABA. In all recordings, a 2.5-minute wash was executed between all applications to prevent receptor desensitization. At the end of each recording on an oocyte, a GABA concentration evoking the maximum response through the specific receptor was applied in the perfusate. Experiments were performed at room temperature, and each data point represents the mean ± S.E.M. value of recordings performed on at least three oocytes from at least two different batches of oocytes.

The recorded baseline-to-peak current amplitudes were analyzed using Clampfit 10.1 (Axon Instruments, Union City, CA), and data for the test compounds were normalized to the maximal response elicited by GABA on each oocyte. Data analysis and statistical analysis were performed using Prism GraphPad, version 6.0a (GraphPad Software, Inc. La Jolla, CA). Concentration-response and concentration-inhibition curves were fitted by nonlinear regression using the equation for sigmoidal dosage-response with variable slope. Comparison of best-fitting equation (monophasic versus biphasic) was carried out using the extra sum-of-squares F test, and the null hypothesis was rejected at $P < 0.05$. When a biphasic fit was the statistically better model, data were fitted to the equation for a biphasic dose-response curve using nonlinear regression. Unless otherwise stated in the figure legends, statistical analysis was performed using ordinary one-way analysis of variance. The null hypothesis was rejected at $P < 0.05$, and the differences between the means were analyzed by Dunnett´s multiple comparisons test with a single pooled variance.

In Silico Study

The modeling study was performed using the software package MOE 2013.08 (Molecular Operating Environment, Chemical Computing Group, Montreal, QC, Canada) using the built-in mmff94x force field and the GB/SA continuum solvation model. Etomidate, loreclezole, and methaqualone were submitted to a stochastic conformational search (standard setup) to enumerate low-energy conformations. Structurally collapsed conformations were discarded, and superimposition of selected low-energy conformations (up to $\Delta\Delta G = 3$ kcal/mol) was done using the built-in function by fitting the carbonyl groups of etomidate and methaqualone and the vinylogous chlorine of loreclezole.

Screening of Methaqualone at Various CNS targets

In vitro binding profiling of methaqualone in competition radiobinding assays at a total of 53 CNS targets were performed by the National Institute of Mental Health's Psychoactive Drug Screening Program (PDSP). Detailed information about the binding assay protocols is given at http://pdsp.med.unc.edu/pdspw/binding.php. In brief, most of the binding assays were performed to homogenates of mammalian cell lines transiently or stably expressing the different targets, with a few assays being performed using homogenized rat brain tissue. Methaqualone was tested in an assay concentration of 30 μM, and an assay concentration of the radioligand near or at the K_D value for the specific target was used. The functional characterization of methaqualone at $GABA_B$ receptors and at the $\alpha_4\beta_2$ nicotinic

acetylcholine receptor in fluorescence-based Ca^{2+}/Fluo-4 or membrane potential assays and at the human four GABA transporters in a conventional [^{3}H]GABA uptake assay was performed essentially as described previously (Trattnig et al., 2012; Hoestgaard-Jensen et al., 2014).

Functional Phenotypic Characterization of Methaqualone at Neuronal Cell Cultures

The effects of methaqualone at cortical network activity in vitro were characterized essentially as previously described for the opioid ligand LP1 (Parenti et al., 2013).

Primary Cell Cultures. Frontal cortex tissue was harvested from embryonic day 15/16 chr:NMRI mice (Charles River, Sulzfeld, Germany). The mice were sacrificed by cervical dislocation according to the German Animal Protection Act §4. Tissue was dissociated by enzymatic digestion (133.3 Kunitz U/ml DNase, 10 U/ml papain) and mechanical trituration, counted, vitality-controlled, and plated in Dulbecco's modified Eagle's medium containing 5% fetal bovine serum and 5% horse serum on poly-D-lysine– and laminin-coated microelectrode array (MEA) neurochips with 64 passive electrodes (Center for Network NeuroScience, University of North Texas, Denton, TX). Cultures on the MEA chips were incubated at 37°C in a 10% CO_2 atmosphere until ready for use, usually 4 weeks after seeding. Culture media were replenished twice a week with Dulbecco's modified Eagle's medium containing 10% horse serum. The developing cocultures were treated with the mitosis inhibitor 5-fluoro-2′-deoxyuridine (25 μM) and uridine (63 μM) for 48 hours on day 5 after seeding to prevent further glial proliferation. After 4 weeks in culture, the activity pattern stabilizes and is composed of one coordinated main burst pattern with several coordinated subpatterns (Gramowski et al., 2004, 2006a,b). In this study, cultures between 28 and 35 days in vitro were used.

Multichannel and Data Analysis. Extracellular recordings were performed using a computer-controlled 64-channel MEA workstation acquisition system (Plexon, Inc., Dallas, TX), where temperature control of 37°C and stable pH of 7.4 (10% CO_2) enabled stable recording and cumulative concentration-response determinations for periods longer than 10 hours (Parenti et al., 2013). The neuronal networks were acutely treated with a series of accumulating increasing concentrations of the test compound (maximum assay concentration of dimethylsulfoxide: 0.1%). For each of the applied test compound concentrations, a stable activity phase of the last 30 minutes was analyzed, and real-time unit separation and spike identification were performed in real time as previously described (Parenti et al., 2013). Action potentials, termed spikes, were recorded as spike trains, which in cortical neurons are clustered in bursts (Gramowski et al., 2006a), and these were quantitatively described via direct spike train analysis using the programs NeuroEXplorer (Plexon Inc., Dallas, TX) and the proprietary tool NPWaveX. Bursts definition and high content analysis of the network activity patterns provided a multiparametric description characterizing the activity changes in four defined categories: overall activity, burst structure, oscillatory behavior and synchronicity (see Parenti et al., 2013) for more information). The parameters for each experiment and each experimental treatment were normalized to the corresponding values of the native reference activity. From each network, 21–158 separate neurons were simultaneously recorded.

Pattern Recognition and Classification. Characteristics of the effects displayed by methaqualone on the activity of cortical networks were elucidated further by analysis of the electrophysiologic data using methods of pattern recognition and cross validation as previously described (Parenti et al., 2013). A total of 204 spike train features were calculated using NPWaveX (NeuroProof GmbH, Rostock, Germany). Activity changes within these 204 features over the tested concentration range generate a functional, phenotypic profile for a compound. Methaqualone data were subsequently classified using pattern recognition (software package PatternExpert, NeuroProof GmbH) by comparison with the phenotypic profiles of 69 reference compounds from the NeuroProof database. An artificial neuronal network was trained with the datasets from the reference compounds to establish a classifier (multilayer feed forward network and back propagation algorithm without hidden units). It uses a multilayer feed-forward perceptron and a resilient-propagation learning algorithm that uses as many input nodes as features and one output node for each class that has to be classified. Relatively high variation of our data justifies nonuse of hidden layers. The thereby obtained cross-validation delivers a ranking that reflects the functional similarity between methaqualone data sets and reference compound. This analysis was repeated 10 times. The values reflect "% of methaqualone datasets classified as a phenotypic reference profile," named the similarity score. High values reflect high functional phenotypic similarity between reference compound profiles and methaqualone.

Animal Studies

Animals. Male NMRI mice (20–24 g at the time of testing) from Charles River (Germany) were housed under controlled conditions (12 hours of light starting at 06:00 hours, 20 ± 2°C, 30–70% humidity) in Macrolon (type III) cages, with standard sawdust bedding and environmental enrichment (plastic house and wooden chew blocks) and food and water available ad libitum. The experiments were carried out in accordance with the Danish legislation regulating animal experiments, Law and Order on Animal experiments; Act no. 474 of 15/05/2014 and Order no. 88 of 30/01/2013, and with the specific license for this experiment issued by the National Authority.

Maximal Electroshock Seizures Threshold and Beam Walk Assays. Methaqualone was tested 60 minutes and diazepam 30 minutes after a subcutaneous dose in the beam walk assay, which is a sensitive measure of sedation or ataxia side effects. Briefly, mice walk across a wooden beam, 8 mm in diameter and 60 cm long, to a goal box at the far end. The number of foot slips and number of falls from the beam are scored (Stanley et al., 2005). The same mouse is first tested in beam walking, and then the convulsion threshold is determined by the maximal electroshock seizures threshold (MEST) to tonic hind limb extension by electrical stimulation via corneal electrodes using the 'up and down' method of shock titration (Kimball et al., 1957; Löscher and Schmidt, 1988). Electrical stimulation was delivered by electrical stimulator (Ellegaard Systems, Faaborg, Denmark) as constant current for 0.4 seconds at 50 Hz starting at 14 mA, and the stimulation intensity was lowered or raised by 2 mA steps if the preceding mouse did or did not show hind limb extension, respectively. In the same mouse, plasma and brain samples were taken to directly link efficacy to exposure.

Plasma and Brain Exposure Analysis. Mouse plasma and brain samples from the MEST study were analyzed for methaqualone using ultra-performance liquid chromatography followed by tandem mass spectrometry detection. Brain homogenate samples were prepared by homogenizing the brain 1:4 (v/v) with water: 2-propanol:dimethylsulfoxide (50:30:20 v/v/v), followed by centrifugation and collection of the supernatant. Sample preparation was performed by protein precipitation with acetonitrile, followed by centrifugation and the addition of 0.1% ammonium hydroxide. The mobile phase consisted of water/acetonitrile with ammonium hydroxide pumped through an analytical column (Acquity ultra performance liquid chromatography BEH phenyl column 1.8 μm, 2.1 × 30 mm, Waters, MA). Detection was performed using a Sciex-API 4000 MS (Applied Biosystems, The Netherlands) using electrospray with positive ionization mode with a parent > daughter molecular mass of 251.1 > 91.1 amu. The lower limit of quantification was 1 ng/ml in plasma and 5 ng/g in brain (peak $S/N > 6$). The free fraction of methaqualone was determined in vitro using standard equilibrium dialysis methods with freshly isolated mouse brain homogenate or plasma (Redrobe et al., 2012). Equilibrium dialysis was performed by incubating at 37°C for 5 hours in triplicate.

Results

Functional Characterization of Methaqualone at Human $GABA_ARs$ Expressed in *Xenopus* Oocytes

The functional properties of methaqualone were characterized at 13 human $GABA_AR$ subtypes expressed in *Xenopus* oocytes by TEVC electrophysiology. Whereas GABA displayed monophasic concentration-response relationships at the most of these receptors, its concentration-response curves at the $\alpha_4\beta_3\delta$ $GABA_AR$ were distinctly biphasic, and recordings from $\alpha_4\beta_1\delta$-oocytes resulted in both monophasic and biphasic concentration-response curves (Table 1). In agreement with previous reports (Karim et al., 2012; Jensen et al., 2013; Hoestgaard-Jensen et al., 2014), the receptors formed in $\alpha_4\beta_1\delta$- and $\alpha_4\beta_3\delta$-expressing oocytes also exhibited pronounced levels of constitutive activity (assessed by application of 10 μM picrotoxin; unpublished data). All in all, these basic functional properties of the receptors were in good agreement with those obtained in previous studies (Mortensen et al., 2011; Karim et al., 2012, 2013; Hoestgaard-Jensen et al., 2013, 2014).

In the initial round of characterization, the functional properties of methaqualone were determined at $\alpha_1\beta_2\gamma_{2S}$, $\alpha_2\beta_2\gamma_{2S}$, $\alpha_3\beta_2\gamma_{2S}$, $\alpha_4\beta_2\delta$, $\alpha_5\beta_2\gamma_{2S}$ and $\alpha_6\beta_2\delta$ $GABA_ARs$ (Fig. 1). This selection of receptors not only represents the full spectrum of molecular diversity in terms of α-subunits but also comprises six major physiologic $GABA_AR$ subtypes (Olsen and Sieghart, 2008; Belelli et al., 2009; Brickley and Mody, 2012). Methaqualone displayed negligible agonism at the $\alpha_{1,2,3,5}\beta_2\gamma_{2S}$ receptors (R_{max} values of 1–4% of GABA R_{max}), whereas it was more efficacious as an agonist at $\alpha_4\beta_2\delta$ ($R_{max} \pm$ S.E.M. = 5.5 ± 1.6%; n = 5) and $\alpha_6\beta_2\delta$ ($R_{max} \pm$ S.E.M. = 13 ± 1.6%; n = 8). In addition to its small intrinsic agonist activity, methaqualone was a PAM exhibiting midmicromolar EC_{50} values at all six receptors when coapplied with GABA EC_{10} (Fig. 1B; Table 1). The currents evoked by GABA EC_{10} in $\alpha_1\beta_2\gamma_{2S}$-, $\alpha_2\beta_2\gamma_{2S}$-, $\alpha_3\beta_2\gamma_{2S}$-, and $\alpha_5\beta_2\gamma_{2S}$ oocytes were potentiated 6- to 8-fold by maximal potentiating concentrations of methaqualone. The compound was an even more efficacious PAM at the $\alpha_4\beta_2\delta$ and $\alpha_6\beta_2\delta$ $GABA_ARs$, potentiating GABA EC_{10}-evoked currents through these receptors to amplitudes 2- to 3-fold greater than the maximal responses of GABA (Fig. 1B; Table 1). Interestingly, methaqualone displayed bell-shaped concentration-response curves as a PAM at all receptors when coapplied with GABA EC_{10} in concentrations ranging from 1 to 1000 μM (exemplified for

TABLE 1

Functional properties of GABA and methaqualone determined by two-electrode voltage-clamp electrophysiology at human $GABA_ARs$ expressed in *Xenopus* oocytes

Unless otherwise indicated in the footnotes to this table, data given for methaqualone represents its properties as a positive allosteric modulator determined at the receptors in the presence of GABA EC_{10}. EC_{50} values are given in μM with $pEC_{50} \pm$ S.E.M. values in brackets, and R_{max} values are given in percentage of the R_{max} value of GABA at the receptor (n indicates number of experiments performed).

	GABA		Methaqualone		
	EC_{50} ($pEC_{50} \pm$ S.E.M.)	n	EC_{50} ($pEC_{50} \pm$ S.E.M.)	$R_{max} \pm$ S.E.M.	n
$\alpha_1\beta_2$	7.8 (5.11 ± 0.05)	6	49 (4.31 ± 0.03)	79 ± 3.7	6
$\alpha_1\beta_2\gamma_{2S}$	57 (4.25 ± 0.10)	6	38 (4.41 ± 0.03)	84 ± 2.1	7
$\alpha_1\beta_3\gamma_{2S}$	34 (4.46 ± 0.18)	5	30 (4.52 ± 0.03)	77 ± 2.2	6
$\alpha_2\beta_2\gamma_{2S}$	40 (4.40 ± 0.07)	4	24 (4.61 ± 0.03)	75 ± 2.1	9
$\alpha_3\beta_2\gamma_{2S}$	120 (3.94 ± 0.03)	7	49 (4.31 ± 0.12)	66 ± 2.4	4
$\alpha_4\beta_1\delta$[a] *monophasic*	0.46 (6.33 ± 0.44)	3	n.d.	n.d.	
$\alpha_4\beta_1\delta$[a] *biphasic*	0.034 (7.47 ± 0.54)				
	1.2 (5.91 ± 0.51)	4	n.d.	n.d.	12[a]
$\alpha_4\beta_2\delta$	2.2 (5.65 ± 0.10)	7	68 (4.17 ± 0.06)	240 ± 27	5
$\alpha_4\beta_3\delta$	0.012 (7.94 ± 0.16)				
	3.1 (5.51 ± 0.14)	5	120 (3.91 ± 0.14)[b]	230 ± 12[b]	6[b,c]
$\alpha_5\beta_2\gamma_{2S}$	31 (4.50 ± 0.06)	6	28 (4.56 ± 0.04)	73 ± 1.6	6
$\alpha_6\beta_1\delta$	1.4 (5.85 ± 0.08)	6	~100 (~4.0)[d]		5[d]
$\alpha_6\beta_2$	0.28 (6.54 ± 0.07)	7	74 (4.13 ± 0.02)	220 ± 25	4
$\alpha_6\beta_2\delta$	0.30 (6.52 ± 0.04]	6	36 (4.44 ± 0.04)	280 ± 22	8
$\alpha_6\beta_3\delta$	0.60 (6.23 ± 0.03)	8	31 (4.50 ± 0.04)	110 ± 21	7
$\alpha_1^{M236W}\beta_2\gamma_{2S}$	4.1 (5.39 ± 0.11)	6	88 (4.06 ± 0.03)[b]	60 ± 4.8[b]	4[b,c]
$\alpha_1\beta_2^{M286W}\gamma_{2S}$	5.4 (5.26 ± 0.07)	6	25 (4.60 ± 0.22)	41 ± 2.6	5
$\alpha_6\beta_1^{S265N}\delta$	0.90 (6.05 ± 0.02)	5	96 (4.02 ± 0.03)	230 ± 24	5[c]
$\alpha_6\beta_2^{N265S}\delta$	0.30 (6.53 ± 0.02)	4	~300 (~3.5)[d]		7[d]

n.d., not determinable.

[a]GABA displayed monophasic and biphasic concentration-response curves at three and four of seven $\alpha_4\beta_1\delta$-expressing oocytes, respectively. Methaqualone was tested as a positive and negative allosteric modulator at both oocyte populations.

[b]Properties of methaqualone as an agonist at $\alpha_4\beta_3\delta$ and $\alpha_1^{M236W}\beta_2\gamma_{2S}$ $GABA_ARs$. Agonist EC_{50} values are given in μM with $pEC_{50} \pm$ S.E.M. values in brackets, and R_{max} values are given in percentage of the R_{max} value of GABA at the receptor.

[c]The concentration-response curve was not completely saturated at the highest methaqualone concentration tested. EC_{50} (pEC_{50}) and R_{max} values have been extracted from the fitted curve.

[d]Properties of methaqualone as a negative allosteric modulator at $\alpha_6\beta_1\delta$ and $\alpha_6\beta_2^{N265S}\delta$ $GABA_ARs$ determined in the presence of GABA EC_{60-70}. Estimated IC_{50} values are given in μM with pIC_{50} in brackets.

$\alpha_1\beta_2\gamma_{2S}$ and $\alpha_6\beta_2\delta$ in Fig. 1, C and D). Furthermore, pronounced rebound currents were observed at methaqualone concentrations of 300 μM and greater (Fig. 1C).

To elucidate the nature of methaqualone-mediated modulation of $\alpha\beta\gamma$ and $\alpha\beta\delta$ $GABA_A$Rs, GABA concentration-relationships at the $\alpha_1\beta_2\gamma_{2S}$ and $\alpha_6\beta_2\delta$ receptors were determined in the absence or presence of the modulator. In agreement with previous studies (Campo-Soria et al., 2006; Gielen et al., 2012), the maximal current amplitude evoked by GABA through $\alpha_1\beta_2\gamma_{2S}$ in the presence of a saturating diazepam concentration (3 μM) (R_{max} ± S.E.M. = 110 ± 10%; n = 4) did not differ significantly from that elicited by GABA alone, whereas the benzodiazepine gave rise to a small but significant (2.4-fold) left shift of the concentration-response curve [EC_{50} (pEC_{50} ± S.E.M.) = 24 μM (4.62 ± 0.10) (n = 4) versus 57 μM (4.25 ± 0.10) (n = 7); $P < 0.1$] (Fig. 1E). In contrast, preincubation and coapplication of 300 μM methaqualone increased the potency of GABA at the receptor by 41-fold [(EC_{50} (pEC_{50} ± S.E.M.) = 1.4 μM (5.85 ± 0.08) (n = 6) versus 57 μM 4.25 ± 0.10] (n = 7); $P < 0.001$), whereas the maximal response evoked by GABA was significantly reduced [R_{max} ± S.E.M. = 82 ± 2.3% (n = 6); $P < 0.1$] (Fig. 1E). Interestingly, it was impossible to determine the effect of 300 μM methaqualone at the GABA concentration-response relationship at the $\alpha_6\beta_2\delta$ receptor, since the large currents elicited through this receptor by coapplications of the modulator and high GABA concentrations consistently resulted in failure to keep the holding potential of the oocytes. However, low GABA concentrations unable to evoke significant currents in $\alpha_6\beta_2\delta$-oocytes when applied alone were observed to induce substantial currents when coapplied with 300 μM methaqualone (unpublished data). Thus, although we were unable to quantify the degree of left shift of the GABA concentration-response curve brought on by the presence of methaqaulone, the drug clearly modulated both GABA potency and efficacy at this receptor.

With the first round of characterization having revealed distinctly different methaqualone functionalities at different α-containing $GABA_A$R subtypes, the second round focused on the putative importance of β subunit identity and of the accessory γ_{2S}/δ subunit for the modulation of $\alpha_1\beta\gamma_{2S}$ and $\alpha_{4,6}\beta\delta$ $GABA_A$Rs. The methaqualone-mediated potentiation of the $\alpha_1\beta\gamma_{2S}$ $GABA_A$R did not appear to be dependent on the presence of γ_{2S} in the receptor, since the functionalities exhibited by the compound at $\alpha_1\beta_2$ and $\alpha_1\beta_2\gamma_{2S}$ receptors did not differ significantly (Fig. 2A; Table 1). Furthermore, substituting β_2 for β_3 in the $\alpha_1\beta\gamma_{2S}$ complex did not change the potency or efficacy of methaqualone as a PAM substantially (Fig. 2A; Table 1).

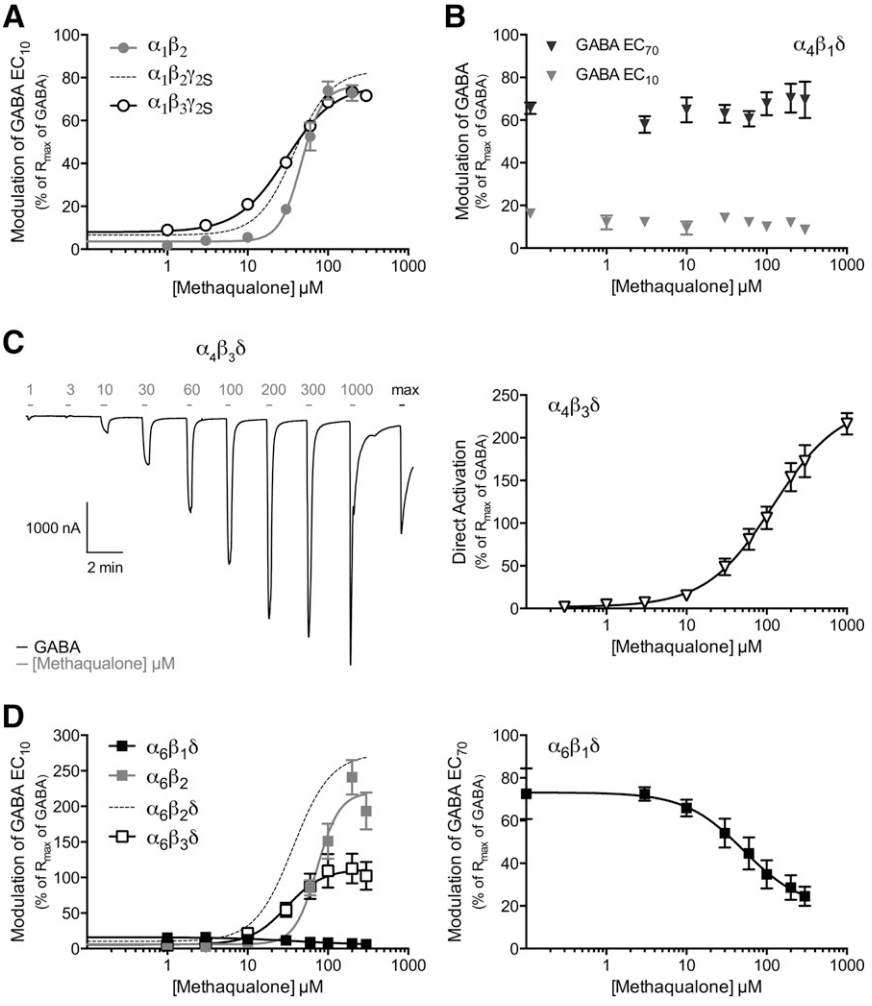

Fig. 2. Functional properties of methaqualone at human $GABA_A$Rs expressed in *Xenopus* oocytes. (A) Concentration-response curves for methaqualone at $\alpha_1\beta_2$, $\alpha_1\beta_2\gamma_{2S}$, and $\alpha_1\beta_3\gamma_{2S}$ $GABA_A$Rs in the presence of GABA EC_{10} (means ± S.E.M.; n = 6–7). (B) Modulation of $\alpha_4\beta_1\delta$ $GABA_A$R signaling exerted by methaqualone in the presence of GABA EC_{10} or GABA EC_{70} (means ± S.E.M.; n = 4–8). (C) Representative trace and the concentration-response curve for methaqualone as an agonist at the $\alpha_4\beta_3\delta$ $GABA_A$R (means ± S.E.M.; n = 6). The gray application bars above the trace indicate application of the various methaqualone concentrations, and the black bar represents the application of a GABA concentration eliciting a maximal response. (D, left) Concentration-response curves for methaqualone at $\alpha_6\beta_2$, $\alpha_6\beta_1\delta$, $\alpha_6\beta_2\delta$, and $\alpha_6\beta_3\delta$ $GABA_A$Rs in the presence of GABA EC_{10} (means ± S.E.M.; n = 4–8). (D, right) Concentration-inhibition curve for methaqualone at the $\alpha_6\beta_1\delta$ $GABA_A$R in the presence of GABA EC_{70} (means ± S.E.M.; n = 5). The hatched concentration-response curves for $\alpha_1\beta_2\gamma_{2S}$ and $\alpha_6\beta_2\delta$ in (A) and (D), respectively, are based on data displayed in Fig. 1B.

In contrast to its comparable modulation of $\alpha_1\beta_2\gamma_{2S}$ and $\alpha_1\beta_3\gamma_{2S}$ receptors, methaqualone displayed dramatically different functionalities at the different β subunit-containing $\alpha_4\beta\delta$ and $\alpha_6\beta\delta$ subtypes. Contrary to its PAM activity at the $\alpha_4\beta_2\delta$ $GABA_AR$ (Fig. 1B), methaqualone did not modulate the responses evoked by GABA EC_{10} or GABA EC_{70} in $\alpha_4\beta_1\delta$-oocytes, and strikingly the presence of β_3 in the $\alpha_4\beta\delta$ complex converted the compound into a superagonist with an efficacy comparable to that of the orthosteric agonist THIP (4,5,6,7-tetrahydroisoxazolo[5,4-*c*]pyridin-3-ol) (Fig. 2, B and C; Table 1) (Storustovu and Ebert, 2006; Hoestgaard-Jensen et al., 2014). The origin of the agonism mediated by methaqualone at this receptor will be addressed further in the *Discussion* section.

The functional properties exhibited by methaqualone at the three $\alpha_6\beta\delta$ $GABA_ARs$ were just as diverse as those at the $\alpha_4\beta\delta$ receptors, but interestingly the pattern of functionalities determined for the modulator at these two receptor groups differed completely (Table 1). Methaqualone was a less efficacious PAM at $\alpha_6\beta_3\delta$ than at the $\alpha_6\beta_2\delta$ $GABA_AR$, and the compound did not potentiate the GABA-evoked signaling through the $\alpha_6\beta_1\delta$ $GABA_AR$ but instead acted as a weak negative allosteric modulator (NAM) at the receptor (Fig. 2D; Table 1). Finally, judging from the similar functional characteristics displayed by methaqualone at $\alpha_6\beta_2$ and $\alpha_6\beta_2\delta$ $GABA_ARs$, the presence of the δ subunit in the $GABA_AR$ assembly did not seem to be important for its modulation of $\alpha\beta\delta$ receptors (Fig. 2D; Table 1).

Delineation of the Mechanism of Action of Methaqualone at the $GABA_AR$

To elucidate the molecular basis for methaqualone modulation of the $GABA_AR$, we investigated the putative interactions of the modulator with four known allosteric sites in the receptor complex.

The Benzodiazepine Site. The high-affinity benzodiazepine site in the $\alpha\beta\gamma$ $GABA_AR$ is located at the extracellular $\alpha^{(+)}/\gamma^{(-)}$ subunit interface (Wieland et al., 1992; Sigel and Lüscher, 2011). Although the similar potencies displayed by methaqualone at the numerous $GABA_AR$ subtypes included in this study suggested that the modulator does not act through this site, the different structure of methaqualone compared with benzodiazepines hypothetically could enable it to bind to the $\alpha^{(+)}/\gamma^{(-)}$ interface in $\alpha\beta\gamma$ receptors, as well as to the corresponding interfaces in $\alpha\beta$ and $\alpha\beta\delta$ $GABA_ARs$. This possibility was investigated by two different approaches.

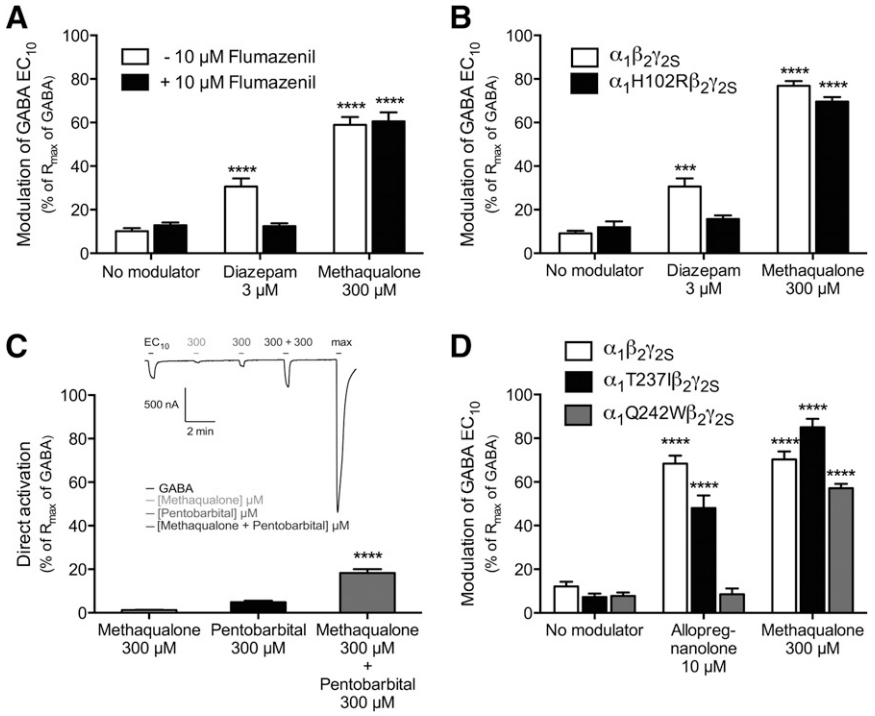

Fig. 3. The potential interaction of methaqualone with three known allosteric sites in the $GABA_AR$ complex. The experiments were performed at human WT and mutant $\alpha_1\beta_2\gamma_{2S}$ $GABA_ARs$ expressed in *Xenopus* oocytes. (A) Effects of 10 μM flumazenil on the potentiation exerted by 3 μM diazepam or 300 μM methaqualone on the responses evoked by GABA EC_{10} through the $\alpha_1\beta_2\gamma_{2S}$ $GABA_AR$. Asterisks indicate significant differences between responses evoked by GABA EC_{10} in the presence of modulator (diazepam and methaqualone) and by GABA EC_{10} alone, either in the absence or presence of flumazenil: $^{****}P < 0.0001$ (means ± S.E.M.; n = 6–13). (B) The modulatory effects of 3 μM diazepam and 300 μM methaqualone on the GABA EC_{10}-evoked responses through $\alpha_1\beta_2\gamma_{2S}$ and $\alpha_1{}^{H102R}\beta_2\gamma_{2S}$ $GABA_ARs$. Asterisks indicate significant differences between responses evoked by GABA EC_{10} in the presence of modulator and by GABA EC_{10} alone at the same receptor (means ± S.E.M.; n = 5–12): $^{***}P < 0.001$; $^{****}P < 0.0001$. (C) Direct activation of the $\alpha_1\beta_2\gamma_{2S}$ $GABA_AR$ evoked by 300 μM methaqualone, by 300 μM pentobarbital, and by coapplication of 300 μM methaqualone and 300 μM pentobarbital (means ± S.E.M.; n = 7). Asterisks indicate the significant difference between the responses evoked by 300 μM pentobarbital and by coapplication of 300 μM methaqualone and 300 μM pentobarbital: $^{****}P < 0.0001$. Insert: Representative trace for direct activation of the $\alpha_1\beta_2\gamma_{2S}$ $GABA_AR$ by 300 μM methaqualone, 300 μM pentobarbital, and coapplication of 300 μM methaqualone and 300 μM pentobarbital. (D) The modulatory effects of 10 μM allopregnanolone and 300 μM methaqualone on the GABA EC_{10}-evoked responses through $\alpha_1\beta_2\gamma_{2S}$, $\alpha_1{}^{T237I}\beta_2\gamma_{2S}$, and $\alpha_1{}^{Q241W}\beta_2\gamma_{2S}$ $GABA_ARs$. Asterisks indicate significant differences between responses evoked by GABA EC_{10} in the presence of modulator and by GABA EC_{10} alone at the same receptor (means ± S.E.M.; n = 4–11): $^{****}P < 0.0001$.

In the first experiment, the effect of the benzodiazepine-site antagonist flumazenil on methaqualone-mediated potentiation of $\alpha_1\beta_2\gamma_{2S}$ receptor signaling was assessed. In concordance with the literature (Sigel and Lüscher, 2011), preincubation and coapplication of 10 μM flumazenil with GABA EC_{10} did not modulate the agonist-evoked response through the receptor significantly (10 ± 1.4% (n = 13) versus 13 ± 1.3% (n = 13)), whereas the potentiation of the GABA EC_{10}-evoked response mediated by 3 μM diazepam (31 ± 3.7%, n = 11) was completely eliminated by the presence of the antagonist (12 ± 1.4%, n = 6) (Fig. 3A). In contrast, 10 μM flumazenil did not reduce the methaqualone-mediated potentiation of $\alpha_1\beta_2\gamma_{2S}$ $GABA_AR$ signaling significantly (59 ± 3.5% (n = 7) versus 61 ± 4.2% (n = 7)) (Fig. 3A).

In the second experiment, the impact of the α_1-H102R mutation on the methaqualone-mediated modulation at $\alpha_1\beta_2\gamma_{2S}$ receptor signaling was investigated. Substitution of this conserved histidine residue in the $\alpha_{1,2,3,5}$-subunit with an arginine (the corresponding residue in $\alpha_{4,6}$) has been shown to render $\alpha_{1,2,3,5}\beta\gamma$ receptors insensitive to benzodiazepines (Wieland et al., 1992; Sigel and Lüscher, 2011). Whereas diazepam (3 μM) was completely inactive as a PAM at the $\alpha_1^{H102R}\beta_2\gamma_{2S}$ $GABA_AR$, the potentiation of GABA EC_{10} evoked-signaling through WT $\alpha_1\beta_2\gamma_{2S}$ and $\alpha_1^{H102R}\beta_2\gamma_{2S}$ receptors exerted by 300 μM methaqualone did not differ substantially (77 ± 2.1% (n = 6) versus 70 ± 2.1% (n = 5)) (Fig. 3B). In conclusion, these findings unequivocally rule out the high-affinity benzodiazepine site as the site of action for methaqualone.

The Barbiturate Site. Although numerous residues and regions in $GABA_ARs$ have been shown to be important for the barbiturate-mediated modulation of the receptors, the exact location of the binding site(s) for these ago-PAMs in the receptors has yet to be identified (Serafini et al., 2000; Greenfield et al., 2002; Feng and Macdonald, 2010; Chiara et al., 2013). To assess whether methaqualone targets the barbiturate site or an overlapping site in the $GABA_AR$, we investigated whether the small but significant agonist response evoked by 300 μM pentobarbital through the $\alpha_1\beta_2\gamma_{2S}$ receptor could be modulated by methaqualone. As can be seen in Fig. 3C, the current amplitudes elicited by 300 μM methaqualone (1.2 ± 0.17%, n = 6) and by 300 μM pentobarbital (4.9 ± 0.68%, n = 6) at $\alpha_1\beta_2\gamma_{2S}$-expressing oocytes were significantly smaller than that arising from coapplication of the two compounds at the receptor (18 ± 1.7%, n = 6). The ability of methaqualone to potentiate pentobarbital-evoked $\alpha_1\beta_2\gamma_{2S}$ signaling demonstrates that it binds to a site that does not overlap with the site through which the barbiturate mediates its direct activation of the receptor. However, in view of the presently limited insight into the molecular basis for barbiturate modulation of $GABA_ARs$, we cannot exclude the possibility that barbiturate-mediated potentiation could arise from a distinct site in the $GABA_AR$ and that this site could overlap with the methaqualone binding site.

The Neurosteroid Sites. Several endogenous and synthetic neurosteroids act as potent ago-PAMs of $GABA_ARs$ (Herd et al., 2007). Smart and coworkers have proposed the existence of two discrete binding sites for neurosteroids in the transmembrane domains of the murine $\alpha_1\beta_2\gamma_2$ $GABA_AR$: an intersubunit site at the $\beta^{(+)}/\alpha^{(-)}$ subunit interface (comprising the α_1-TM1 residue Thr^{236}) important for neurosteroid activation and an intrasubunit site in the α subunit (comprising the α_1-TM1 residue Gln^{241}), which is important for both neurosteroid-mediated potentiation and activation (Hosie et al., 2006, 2009). To investigate whether methaqualone mediates its effects on $GABA_AR$ signaling through one or both of these sites, the impact of mutations of these two α_1 residues (Thr^{237} and Gln^{242}, human α_1 numbering) on the modulation exerted by the compound at the $\alpha_1\beta_2\gamma_{2S}$ $GABA_AR$ was determined. Allopregnanolone was used as reference compound in these recordings, and in concordance with previous studies, the neurosteroid was an efficacious PAM of the $GABA_AR$ (Fig. 3D). In contrast to previous findings, however, allopregnanolone did not exhibit significant intrinsic agonist activity at the receptor at concentrations up to 10 μM (Hosie et al., 2006, 2009; Chen et al., 2014). The possible reasons for the absence of the direct activation component of allopregnanolone at the receptor are currently being investigated in our laboratory.

The absence of allopregnanolone-evoked agonism at the $\alpha_1\beta_2\gamma_{2S}$ receptor obviously precluded us from verifying the previously reported effects of α_1-Q242W and α_1-T237I mutations on this activity component of the neurosteroid. However, in agreement with the previously reported importance of a highly conserved Gln residue in TM1 of the α subunit for neurosteroid-mediated potentiation of $GABA_ARs$ (Hosie et al., 2006, 2009), allopregnanolone was completely inactive as a PAM at the $\alpha_1^{Q242W}\beta_2\gamma_{2S}$ receptor at concentrations up to 10 μM (Fig. 3D). In contrast, the presence of 10 μM allopregnanolone potentiated GABA EC_{10}-evoked currents in WT $\alpha_1\beta_2\gamma_{2S}$- and $\alpha_1^{T237I}\beta_2\gamma_{2S}$-expressing oocytes to similar degrees, which is also in agreement with the findings by Hosie et al. (2006) and with the notion of the proposed intersubunit site being responsible for neurosteroid-mediated activation exclusively (Fig. 3D). Interestingly, the degree of potentiation of the GABA EC_{10}-evoked response through the $\alpha_1\beta_2\gamma_{2S}$ receptor mediated by 300 μM methaqualone was not changed significantly by the introduction of neither the Q242W nor the T237I mutation in the α_1 subunit (Fig. 3D).

Although the functional implications of the two α_1 mutations on allopregnanolone-mediated potentiation of the $GABA_AR$ observed in this study are in concordance with those reported by the Smart group, the apparent discrepancy between our findings and the literature when it comes to the intrinsic agonist activity of the neurosteroid should obviously be kept in mind when interpreting the results obtained for methaqualone in these recordings. We propose that the dramatically different effects induced by the α_1-Q242W mutation on the allopregnanolone- and methaqualone-mediated potentiation of $\alpha_1\beta_2\gamma_{2S}$ receptor signaling unequivocally demonstrate that methaqualone does not act through the proposed intrasubunit neurosteroid site in the receptor. As for the proposed intersubunit neurosteroid site, the lack of intrinsic agonist activity of allopregnanolone at $\alpha_1\beta_2\gamma_{2S}$ clearly devaluates it as a reference compound. Taken at face value, however, the WT-like properties exhibited by methaqualone at the $\alpha_1^{T237I}\beta_2\gamma_{2S}$ receptor does suggest that the modulator does not target a site comprising this residue.

The Transmembrane $\beta^{(+)}/\alpha^{(-)}$ Subunit Interface. The transmembrane $\beta^{(+)}/\alpha^{(-)}$ interface in the $GABA_AR$ harbors binding sites for numerous allosteric modulators, but with the exception of the site targeted by the general anesthetic etomidate

the compositions and locations of these sites are poorly elucidated (Wafford et al., 1994; Belelli et al., 1997; Hill-Venning et al., 1997; Halliwell et al., 1999; Walters et al., 2000; Krasowski et al., 2001; Bali and Akabas, 2004; Thompson et al., 2004; Khom et al., 2007). Interestingly, however, several of these modulators exhibit distinct selectivity between $GABA_AR$ subtypes on the basis of their respective β-subunits (Wafford et al., 1994; Belelli et al., 1997; Hill-Venning et al., 1997; Halliwell et al., 1999; Thompson et al., 2004; Khom et al., 2007). In this light, the differential functionalities displayed by methaqualone at the different β-subunit containing $\alpha_4\beta\delta$ and $\alpha_6\beta\delta$ receptors were intriguing and prompted us to probe the putative importance of three transmembrane residues in the $GABA_AR$ for the functional properties of methaqualone.

Residue 265 in TM2 of the β-subunit (β_1-Ser^{265}, β_2/β_3-Asn^{265}) is a key molecular determinant of the β-selectivity (β_2/β_3-over-β_1 or β_1-over-β_2/β_3) displayed by several of the $\beta^{(+)}/\alpha^{(-)}$ interface modulators (Wingrove et al., 1994; Belelli et al., 1997; Hill-Venning et al., 1997; Halliwell et al., 1999; Khom et al., 2007). In the case of etomidate, the residue is believed not to participate in binding but rather to act as a transduction element between modulator binding and its effect on gating (Li et al., 2006; Desai et al., 2009; Chiara et al., 2012; Stewart et al., 2013; Stewart et al., 2014). In agreement with previous studies (Belelli et al., 1997; Siegwart et al., 2002; Desai et al., 2009; Stewart et al., 2014), the introduction of a N265M mutation in β_2 eliminated etomidate-mediated potentiation of $\alpha_1\beta_2\gamma_{2S}$ receptor signaling completely, and interestingly the mutation had a similar detrimental effect on

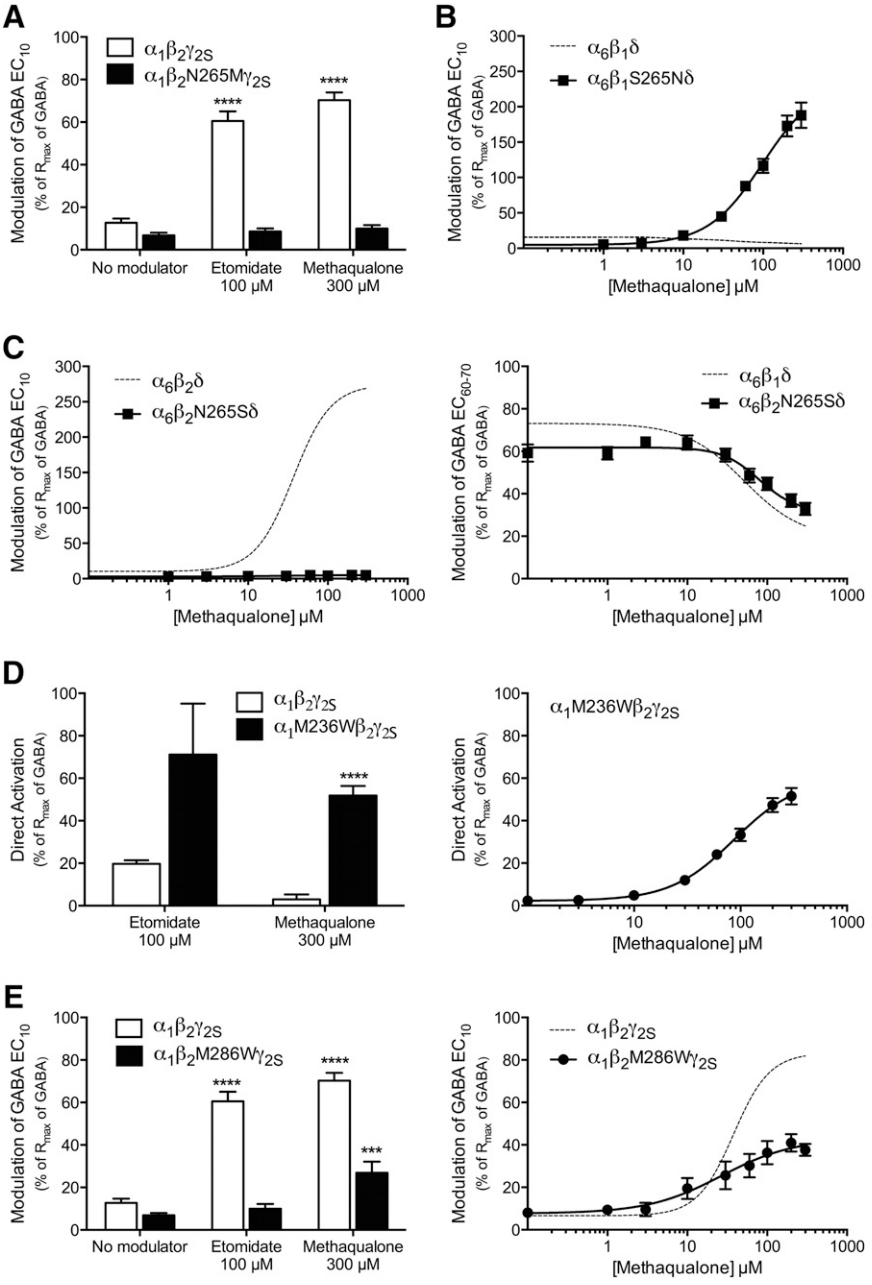

Fig. 4. The potential interaction of methaqualone with the transmembrane $\beta^{(+)}/\alpha^{(-)}$ subunit interface in the $GABA_AR$ complex. The experiments were performed at human WT and mutant $GABA_ARs$ expressed in *Xenopus* oocytes. (A) Modulatory effects of 100 μM etomidate and 300 μM methaqualone on the responses evoked by GABA EC_{10} through $\alpha_1\beta_2\gamma_{2S}$ or $\alpha_1\beta_2^{N265M}\gamma_{2S}$ $GABA_ARs$ (means ± S.E.M.; n = 3–14). Asterisks indicate significant differences between the responses evoked by GABA EC_{10} in the presence of modulator and by GABA EC_{10} alone at the same receptor: ****$P < 0.0001$. (B) Concentration-response curves for methaqualone at $\alpha_6\beta_2\delta$ and $\alpha_6\beta_2^{S265N}\delta$ $GABA_ARs$ in the presence of GABA EC_{10} (means ± S.E.M.; n = 5). (C, left) Concentration-response curves for methaqualone at $\alpha_6\beta_2\delta$ and $\alpha_6\beta_2^{N265S}\delta$ $GABA_ARs$ in the presence of GABA EC_{10} (means ± S.E.M.; n = 3–8). (C, right) Concentration-inhibition curves for methaqualone at $\alpha_6\beta_1\delta$ and $\alpha_6\beta_2^{N265S}\delta$ $GABA_ARs$ in the presence of GABA $EC_{60\text{-}70}$ (means ± S.E.M.; n = 5–7). (D, left) Direct activation of $\alpha_1\beta_2\gamma_{2S}$ and $\alpha_1\beta_2^{M236W}\gamma_{2S}$ $GABA_AR$ signaling evoked by 100 μM etomidate and 300 μM methaqualone (means ± S.E.M.; n = 4–8). Asterisks indicate significant differences between the responses evoked by etomidate or methaqualone at the two receptors: ****$P < 0.0001$ (unpaired two-sided t test). (D, right) Concentration-response curve for methaqualone as an agonist at the $\alpha_1\beta_2^{M236W}\gamma_{2S}$ $GABA_AR$ (mean ± S.E.M.; n = 4). (E, left) Modulatory effects of 100 μM etomidate and 300 μM methaqualone on the responses evoked by GABA EC_{10} at $\alpha_1\beta_2\gamma_{2S}$ and $\alpha_1\beta_2^{M286W}\gamma_{2S}$ $GABA_ARs$ (means ± S.E.M.; n = 3–10). Asterisks indicate significant differences between the responses evoked by GABA EC_{10} in the presence of modulator and by GABA EC_{10} alone at the same receptor: ****$P < 0.0001$; ***$P < 0.001$. (E, right) Concentration-response curves for methaqualone at $\alpha_1\beta_2\gamma_{2S}$ and $\alpha_1\beta_2^{M286W}\gamma_{2S}$ $GABA_ARs$ in the presence of GABA EC_{10} (means ± S.E.M.; n = 5–7). The hatched concentration-response curves for $\alpha_6\beta_1\delta$ (B) $\alpha_6\beta_2\delta$ (C) and $\alpha_1\beta_2\gamma_{2S}$ (E) are based on data in Figs. 2D, 1B, and 1B, respectively.

the methaqualone-mediated potentiation (Fig. 4A). Furthermore, the PAM and NAM activities exhibited by methaqualone at the $\alpha_6\beta_2\delta$ and $\alpha_6\beta_1\delta$ receptors, respectively, were completely reversed by the introduction of the reciprocal residue in position 265 of the respective β subunits. In fact, methaqualone was roughly equipotent and equally efficacious as a PAM at the $\alpha_6\beta_2\delta$ and $\alpha_6\beta_1{}^{S265N}\delta$ receptors and as a NAM at the $\alpha_6\beta_1\delta$ and $\alpha_6\beta_2{}^{N265S}\delta$ receptors (Fig. 4, B and C; Table 1).

Elaborate photolabeling, substituted cysteine accessibility method, and mutagenesis studies have demonstrated the key importance of the α1-TM1 Met^{236} and β2-TM3 Met^{286} residues for the $GABA_AR$ modulation exerted by etomidate, and the two residues are believed to form direct interactions with the modulator (Siegwart et al., 2002; Li et al., 2006; Stewart et al., 2008; Chiara et al., 2012; Stewart et al., 2013). In concordance with previous studies (Siegwart et al., 2002; Stewart et al., 2008), etomidate (100 μM) displayed higher intrinsic agonist activity at the $\alpha_1{}^{M236W}\beta_2\gamma_{2S}$ $GABA_AR$ than at the WT $\alpha_1\beta_2\gamma_{2S}$ receptor, whereas it was completely inactive at the $\alpha_1\beta_2{}^{M286W}\gamma_{2S}$ receptor (Fig. 4, D and E). Analogously to the increased intrinsic agonist activity of etomidate brought on by the α_1-M236W mutation, the insignificant agonism of methaqualone at WT $\alpha_1\beta_2\gamma_{2S}$ was converted into pronounced agonist activity at the $\alpha_1{}^{M236W}\beta_2\gamma_{2S}$ receptor (Fig. 4D). Conversely, the effect of the β_2-M286W mutation on methaqualone functionality was considerably more subtle than that for etomidate, methaqualone being roughly equipotent albeit less efficacious as a PAM at the $\alpha_1\beta_2{}^{M286W}\gamma_{2S}$ $GABA_AR$ compared with the WT receptor (Fig. 4E).

In a final experiment, we compared the modulation exerted by etomidate at the $\alpha_4\beta\delta$ $GABA_ARs$ with the diverse functionalities exhibited by methaqualone at the three receptors. As mentioned previously, etomidate acts as a PAM at a plethora of $\alpha_{1,2,3,6}\beta\gamma_2$ $GABA_ARs$, being ~10-fold more potent and substantially more efficacious at β_2-/β_3-containing than at β_1-containing subtypes of these receptors (Belelli et al., 1997; Hill-Venning et al., 1997). Etomidate has also been reported to potentiate GABA-evoked signaling through $\alpha_4\beta_3\delta$ $GABA_ARs$ expressed in *Xenopus* oocytes and in mammalian cell lines (Brown et al., 2002; Meera et al., 2009; Jensen et al., 2013), but to our knowledge, its modulatory effects at recombinant $\alpha_4\beta_1\delta$ and $\alpha_4\beta_2\delta$ receptors have not been reported. Etomidate (100 μM) displayed no significant agonist activity at the receptors formed in $\alpha_4\beta_1\delta$-expressing oocytes and only slightly higher intrinsic activity at the $\alpha_4\beta_2\delta$ $GABA_AR$ (R_{max} values of 1–5% of GABA R_{max}). However, the compound robustly potentiated GABA EC_{10}-evoked responses through the two receptors (Fig. 5A). Conversely, etomidate (100 μM) was a pronounced agonist at the $\alpha_4\beta_3\delta$ $GABA_AR$, evoking a response ~4-fold higher than the GABA R_{max} at the receptor (Fig. 5B). Although the fact that we only studied the effects of a single high etomidate concentration (100 μM) in these recordings combined with its reported bell-shaped concentration-response relationships at other $GABA_ARs$ (Belelli et al., 1997; Hill-Venning et al., 1997) preclude us from drawing conclusions regarding whether etomidate exhibits differential modulatory potencies or efficacies at the three $\alpha_4\beta\delta$ receptors, the qualitative nature of its modulation of the receptors can be extracted from the data. Analogously to methaqualone, etomidate is a fairly pure PAM at $\alpha_4\beta_2\delta$ and a superagonist at the $\alpha_4\beta_3\delta$ receptor, whereas its PAM activity at the $\alpha_4\beta_1\delta$ $GABA_AR$ contrasts the inactivity of methaqualone at this subtype (at concentrations up to 300 μM).

Putative Binding Modes of Etomidate, Loreclezole, and Methaqualone. All in all, the results outlined above indicate that methaqualone acts through the same transmembrane $\beta^{(+)}/\alpha^{(-)}$ interface in the $GABA_AR$ complex targeted by etomidate, the anticonvulsant drug loreclezole, and several other modulators. An analysis of the physical-chemical properties of etomidate, loreclezole, and methaqualone shows that the three compounds share notable structural similarities. Both etomidate and methaqualone comprise two hydrophobic moieties, as well as a carbonyl group and an aromatic nitrogen capable of acting as hydrogen bond acceptors (Fig. 6A). Loreclezole comprises one hydrophobic moiety as well as a vinylogous chlorine and a triazole ring system as a potential hydrogen bond acceptors (Fig. 6A). This similarity prompted us to compare the putative binding modes of the three modulators with the aim of defining one common pharmacophore.

In view of the relatively high functional potencies of etomidate, loreclezole, and methaqualone as $GABA_AR$ modulators, all three modulators are expected to bind to the receptor in a low-energy conformation. Thus, the three molecules were initially submitted to a stochastic conformational search to enumerate their respective low-energy conformations. In the

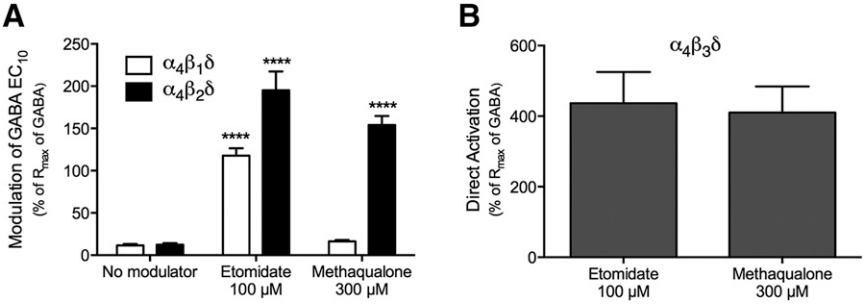

Fig. 5. Functional properties of 100 μM etomidate at human $\alpha_4\beta\delta$ $GABA_ARs$ expressed in *Xenopus* oocytes. The modulation exerted by etomidate and methaqualone was determined at the same $\alpha_4\beta_1\delta$-, $\alpha_4\beta_2\delta$-, or $\alpha_4\beta_3\delta$-expressing oocytes. (A) Modulatory effects of 100 μM etomidate and 300 μM methaqualone on the responses evoked by GABA EC_{10} through $\alpha_4\beta_1\delta$ or $\alpha_4\beta_2\delta$ $GABA_ARs$. Responses given as means ± S.E.M. in the percentage of R_{max} of GABA; etomidate: 118 ± 9% ($\alpha_4\beta_1\delta$; $n = 6$) and 195 ± 23% ($\alpha_4\beta_2\delta$, $n = 4$); methaqualone: 16% ± 1.7 ($\alpha_4\beta_1\delta$; $n = 6$) and 154 ± 11% ($\alpha_4\beta_2\delta$, $N = 4$). ****$P <$ 0.0001. (B) Direct activation of the $\alpha_4\beta_3\delta$ $GABA_AR$ by 100 μM etomidate or 300 μM methaqualone. Responses given as means ± S.E.M. in percentage of R_{max} of GABA; etomidate: 410 ± 88%; $n = 6$; methaqualone: 437 ± 74%; $n = 6$.

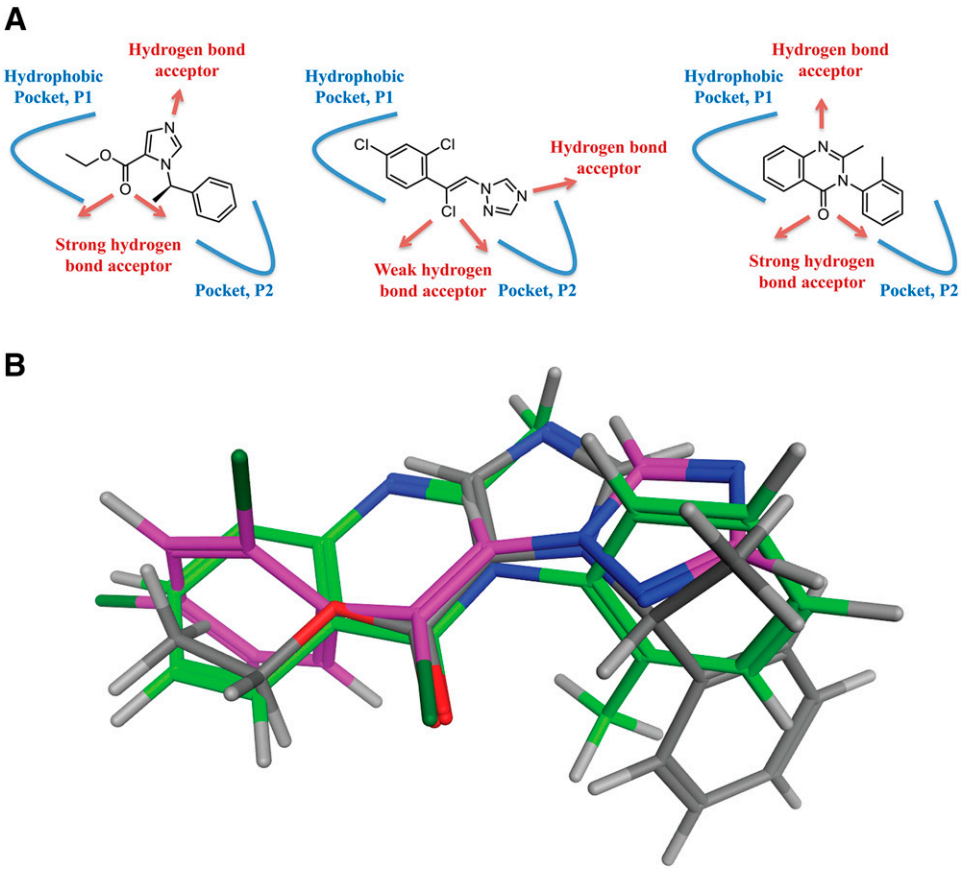

Fig. 6. The putative shared binding mode of etomidate, loreclezole, and methaqualone. (A) Illustration of the structural similarities between etomidate (left), loreclezole (middle), and methaqualone (right). The putative pockets P1 and P2 are given in blue, and the hydrogen bond acceptors in the compounds are indicated with red arrows. (B) Superimposition of low-energy conformations of etomidate (type code), loreclezole (pink), and methaqualone (green) by fitting the carbonyl groups of etomidate and methaqualone and the vinylogous chlorine of loreclezole.

case of etomidate, the 2-phenethyl group adapted only one well defined conformation, and although three rotamers of the ester alkyl group was found the energy differences between these were not significant (<1 kcal/mol). Methaqualone is also a highly rigid molecule, and its low-energy conformation was readily determined. The same was true for loreclezole, which adapted only one low-energy conformation. The low-energy conformations of the three molecules were superimposed based on the assumption that carbonyl groups of etomidate and methaqualone and the vinylogous chlorine of loreclezole dictate the binding modes of the respective compounds in the putative shared site (Fig. 6B). From this overlay, it is clear that the ester alkyl group of etomidate, the 2,4-diclorophenyl ring of loreclezole, and the fused phenyl ring of methaqualone occupy the same area of space (designated hydrophobic pocket P1 in Fig. 6A). The 2-phenethyl group of etomidate and the *N*-phenyl group of methaqualone are oriented in the same area of space (designated pocket P2 in Fig. 6A). In this area, loreclezole comprises a triazole ring, which in comparison with the corresponding moieties in etomidate and methaqualone is less hydrophobic. Thus, the P2 pocket may be capable of accommodating the binding of ring systems with quite different physicochemical properties. Finally, the aromatic nitrogen atoms in the three molecules do not align perfectly in this superimposition; however, reorganization of the water molecules in the binding pocket (induced fit) could possibly adjust for the differences in hydrogen bond donating trajectories of the respective nitrogen atoms. Thus, the in silico study seems to support the hypothesis that etomidate, loreclezole, and methaqualone could bind to a common site in the transmembrane $\beta^{(+)}/\alpha^{(-)}$ interface of the $GABA_AR$, although it should be noted that the superimposition of etomidate and methaqualone is more successful than the loreclezole/etomidate and loreclezole/methaqualone superimpositions.

Screening of Methaqualone at Other Putative CNS Targets

The possible existence of other CNS targets for methaqualone than $GABA_ARs$ was investigated in an elaborate screening of the compound at a total of 50 recombinant neurotransmitter receptors and transporters and at native $GABA_ARs$ and ionotropic glutamate receptors in rat brain homogenates, a selection that includes numerous key targets for known psychotropic drugs and psychostimulants. For most of these targets, the putative activity of methaqualone was assessed in competition binding assays (performed by PDSP), where radioligand concentrations near or at the K_D value for the specific target in these assays was used to facilitate the detection of both inhibition and potentiation of radioligand binding by the test compound. Methaqualone (30 μM) did not display significant modulation (neither potentiation or inhibition) of radioligand binding to a wide range of serotonin, dopamine, norepinephrine, histamine, acetylcholine, glutamate, opioid, cannabinoid, and sigma receptors or at the three monoamine transporters in these assays (Table 2). Furthermore, the compound was inactive at concentrations up to 1 mM when tested in functional assays at the other plasma membrane-bound targets for GABA: the $GABA_B$ receptors and GABA transporters (Table 2).

The inability of 30 μM methaqualone to compete with [^{3}H]muscimol and [^{3}H]flunitrazepam binding to rat brain

TABLE 2

Pharmacologic properties of methaqualone at various central nervous system targets

The binding affinities for methaqualone at numerous targets in a competition binding assays (using radioligand concentrations near or at the K_D value for the specific target) were determined by National Institute of Mental Health's PDSP. The IC_{50} values obtained for methaqualone in the binding assays are given in micromolar, and percent inhibition or percent potentiation of radioligand binding at 30 μM methaqualone is given in parentheses (positive and negative values represent percent inhibition and percent potentiation of control, respectively). An inhibition of >50% is considered significant by the PDSP. The data are based on four independent determinations. The functional properties of methaqualone at selected transporters and receptors were determined in in-house functional assays and are indicated by the # symbol. The IC_{50} and EC_{50} values obtained for methaqualone in these functional assays are given in micromolar.

Target	Assay	IC_{50} [μM] (% Inhibition)
Serotonin		
5-HT_{1A} (h)	[^{3}H]8-OH-DPAT binding	>30 (6.3)
5-HT_{1B} (h)	[^{3}H]GR125743 binding	>30 (−1.3)
5-HT_{1D} (h)	[^{3}H]GR125743 binding	>30 (7.6)
5-HT_{1e} (h)	[^{3}H]5-HT binding	>30 (−11)
5-HT_{2A} (h)	[^{3}H]Ketanserin binding	>30 (-2.1)
5-HT_{2B} (h)	[^{3}H]LSD binding	>30 (−8.3)
5-HT_{2C} (h)	[^{3}H]Mesulergine binding	>30 (3.3)
5-HT_3A (h)	[^{3}H]LY278584 binding	>30 (−7.7)
5-HT_{5a} (h)	[^{3}H]LSD binding	>30 (−11)
5-HT_6 (h)	[^{3}H]LSD binding	>30 (3.6)
5-HT_7 (h)	[^{3}H]LSD binding	>30 (0.9)
SERT (h)	[^{3}H]Citalopram binding	>30 (−1.5)
Dopamine		
D_1 (h)	[^{3}H]SCH23390 binding	>30 (−2.4)
D_2 (h)	[^{3}H]*N*-Methylspiperone binding	>30 (30)
D_3 (h)	[^{3}H]*N*-Methylspiperone binding	>30 (9.9)
D_4 (h)	[^{3}H]*N*-Methylspiperone binding	>30 (10)
D_5 (h)	[^{3}H]SCH23390 binding	>30 (11)
DAT (h)	[^{3}H]WIN35428 binding	>30 (28)
Norepinephrine		
α_{1A} (h)	[^{3}H]Prazosin binding	>30 (−12)
α_{1B} (h)	[^{3}H]Prazosin binding	>30 (5.6)
α_{1D} (h)	[^{3}H]Prazosin binding	>30 (47)
α_{2A} (h)	[^{3}H]Rauwolscine binding	>30 (45)
α_{2B} (h)	[^{3}H]Rauwolscine binding	>30 (3.4)
α_{2C} (h)	[^{3}H]Rauwolscine binding	~30 (63)
β_1 (h)	[^{125}I]Pindolol binding	>30 (−5.8)
β_2 (h)	[^{3}H]CGP 12177 binding	>30 (−9.4)
β_3 (h)	[^{3}H]CGP 12177 binding	>30 (23)
NET (h)	[^{3}H]Nisoxetine binding	>30 (2.3)
Histamine		
H_1 (h)	[^{3}H]Pyrilamine binding	>30 (31)
H_3 (h)	[^{3}H]α-methylhistamine binding	>30 (−9.5)
Acetylcholine		
m_1 (h)	[^{3}H]QNB binding	>30 (−9.5)
m_2 (h)	[^{3}H]QNB binding	>30 (−4.8)
m_3 (h)	[^{3}H]QNB binding	>30 (−13)
m_4 (h)	[^{3}H]QNB binding	>30 (−17)
m_5 (h)	[^{3}H]QNB binding	>30 (13)
$\alpha 4\beta 2$ (m)#	FLIPR membrane potential sasay	EC_{50} > 1000, IC_{50} > 1000
GABA		
Rat forebrain	[^{3}H]Muscimol binding	>30 (−8.9)
Rat brain	[^{3}H]Flunitrazepam binding	>30 (−11)
Rat peripheral benzodiazepine receptor	[^{3}H]PK11195 binding	>30 (21)
GAT1 (h)#	[^{3}H]GABA uptake	>1000
BGT1 (h)#	[^{3}H]GABA uptake	>1000
GAT2 (h)#	[^{3}H]GABA uptake	>1000
GAT3 (h)#	[^{3}H]GABA uptake	>1000
$GABA_{B1a,2}$ (r)#	Ca^{2+}/Fluo4 assay (with Gqi5)	EC_{50} > 1000, IC_{50} > 1000
$GABA_{B1b,2}$ (r)#	Ca^{2+}/Fluo4 assay (with Gqi5)	EC_{50} > 1000, IC_{50} > 1000
Glutamate		
Rat brain NMDA-R	[^{3}H]MK801 binding	>30 (8.1)
Rat brain AMPA-R	[^{3}H]AMPA binding	>30 (23)
Rat brain KA-R	[^{3}H]KA binding	>30 (18)
Opioid		
δ (h)	[^{3}H]DADLE binding	>30 (34)
κ (h)	[^{3}H]U69593 binding	>30 (4.9)
μ (h)	[^{3}H]DAMGO binding	~30 (50)
Cannabinoid		
CB1 (h)	[^{3}H]CP55940 binding	~30 (54)
CB2 (h)	[^{3}H]CP55940 binding	>30 (6.6)
Sigma		
Sigma1 (rat brain)	[^{3}H]Pentazocine(+) binding	>30 (−16)
Sigma2 (rat, PC12)	[^{3}H]DTG binding	>30 (49)

CGP 12177, 4-[3-(tert-butylamino)-2-hydroxypropoxy]-1,3-dihydrobenzimidazol-2-one; CP55940, 2-[(1*R*,2*R*,5*R*)-5-hydroxy-2-(3-hydroxypropyl)cyclohexyl]-5-(2-methyloctan-2-yl) phenol; GR125743, *N*-[4-methoxy-3-(4-methylpiperazin-1-yl)phenyl]-3-methyl-4-(pyridin-4-yl)benzamide; h, human; LY278584, 1-methyl-*N*-[(1*R*,5*S*)-8-methyl-8-azabicyclo[3.2.1] octan-3-yl]indazole-3-carboxamide; m, mouse; PK11195, *N*-butan-2-yl-1-(2-chlorophenyl)-*N*-methylisoquinoline-3-carboxamide; r, rat; SCH23390, 8-chloro-3-methyl-5-phenyl-1,2,4,5-tetrahydro-3-benzazepin-7-ol; U69593, *N*-methyl-2-phenyl-*N*-[(5*R*,7*S*,8*S*)-7-pyrrolidin-1-yl-1-oxaspiro[4.5]decan-8-yl]acetamide; WIN35428, methyl (1*S*,3*S*,4*S*,5*R*)-3-(4-fluorophenyl)-8-methyl-8-azabicyclo[3.2.1]octane-4-carboxylate.

tissue in the PDSP screening is in concordance with the binding site proposed for the modulator at $GABA_ARs$ in this study. On the other hand, the insignificant modulation exerted by the compound on radioligand binding to native $GABA_ARs$ in these assays could be argued to contrast with the augmentation of radioligand binding to the orthosteric and the benzodiazepine binding sites in native $GABA_ARs$ previously reported for other allosteric modulators of these receptors. Most notably in connection with methaqualone, both etomidate and loreclezole have been reported to enhance [^{3}H]muscimol and [^{3}H]flunitrazepam binding to rat brain tissue (Quast and Brenner, 1983; Slany et al., 1995; Ghiani et al., 1996; Xue et al., 1996; Zhong and Simmonds, 1997; Sarantis et al., 2008). However, not all modulators targeting a common binding site may necessarily be capable of modulating ligand binding to other sites in the receptors. Furthermore, the reported degrees of radioligand binding enhancement induced by etomidate and loreclezole in these studies vary considerably, and the modulation has not been observed in all studies (Green et al., 1996). Thus, specific assay conditions seem to influence whether putative modulation of binding is detected in a radioligand binding assay.

An obvious caveat connected to the use of the competition binding assays in this screening is that not all ligands targeting an allosteric site in a certain target necessarily will compete with or modulate orthosteric radioligand binding to it. However, most targets assayed by radioligand binding in the screening were family A 7-transmembrane receptors (i.e., 37 of 48), and to our knowledge few (if any) allosteric modulators of these receptors have been reported not to affect orthosteric radioligand binding (Keov et al., 2011). Hence, although we cannot completely exclude the possibility that methaqualone could target an allosteric site in one (or several) of the receptors, the inactivity of the drug in the binding assays is likely to be a true reflection of its pharmacology at these receptors. In contrast, identification of ligands targeting multidomain receptor complexes such as the $GABA_ARs$ or ionotropic glutamate receptors in a competition binding assay is likely to be more dependent on the specific radioligand and the experimental conditions used. Thus, the observed lack of effect of methaqualone on radioligand binding to these receptors should be seen only as a demonstration of the compound not binding to the specific site in the receptor complex targeted by the radioligand.

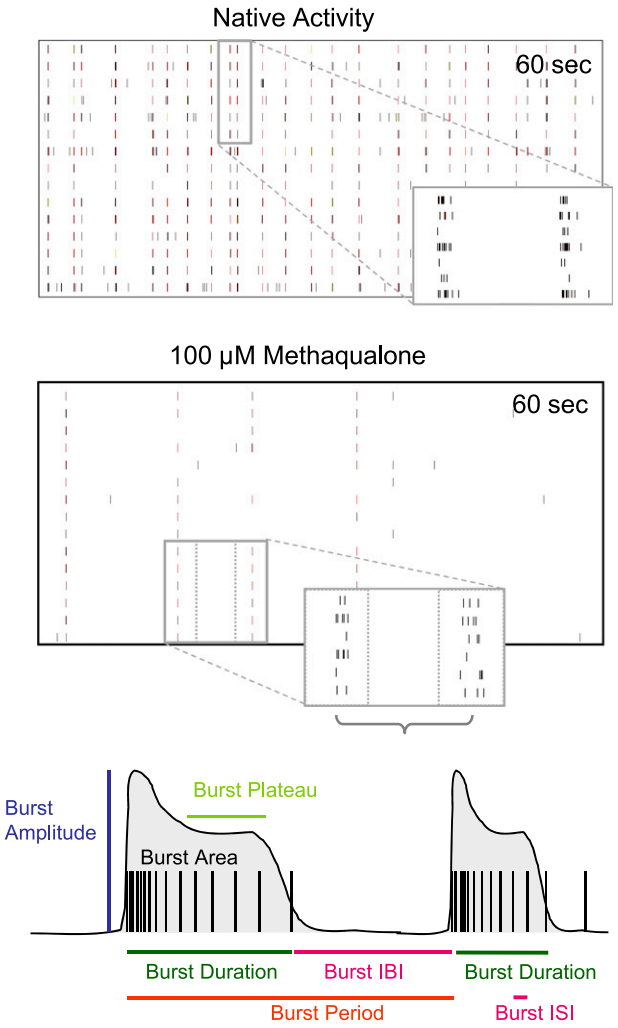

Fig. 7. Multiparametric analysis of cortical neuron network activity. Top panels: Representative spike raster plots of native cortical activity and cortical activity after acute treatment with 100 μM methaqualone. Reduction of overall spiking and bursting activity, as well as reduction of burst strength is observed (higher magnification). Bottom panel: Scheme of two simplified bursts outlining some of the parameters that can be extracted from the recordings. Parameters describing general activity [burst inter burst interval (IBI) and burst period] and burst structure [burst duration, burst plateau, burst amplitude, burst inter spike interval (ISI) and burst area] are indicated. Standard deviations of these parameters such as S.D. of burst rate and S.D. of burst duration are measures for regularity of general activity and burst structure, respectively.

Multiparametric Description of the Effects of Methaqualone on Cortical Network Activity In Vitro

To investigate the effects of methaqualone at native $GABA_ARs$ and on neuronal network activity, we analyzed the modulation exerted by the drug at the spontaneous activity pattern of primary neuronal networks from murine frontal cortex grown on MEA neurochips by multiparametric data analysis. This technology has previously been used extensively for neurotoxicity studies (Gramowski et al., 2006b; Johnstone et al., 2010; Novellino et al., 2011) but also for functional phenotypic screening of drugs (Gramowski et al., 2004, 2006a; Parenti et al., 2013). The 204 activity-describing parameters calculated based on the spike trains from these recordings can be divided into four categories. "General Activity" parameters represent global network activity descriptors such as spike rate, burst rate, percentage of spikes in bursts and burst period; "Burst Structure" parameters describe the internal structure of spikes within a high-frequency spiking phase (e.g., spike frequency in bursts, spike rate in bursts, spike density), as well as the overall burst structure (e.g., duration, area, plateau); "Oscillatory Behavior" parameters are the standard deviations associated with main general activity and burst structure parameters and illustrate the regularity of bursting events within experimental episodes, with higher values indicating less regular general activity or less regular burst structure. Finally, the "Synchronicity" parameters include those representing the coefficient of variation over the network, thus reflecting the level of synchronization among the neurons. Representative spike raster plots and some of the aforementioned extractable parameters from these recordings are given in Fig. 7.

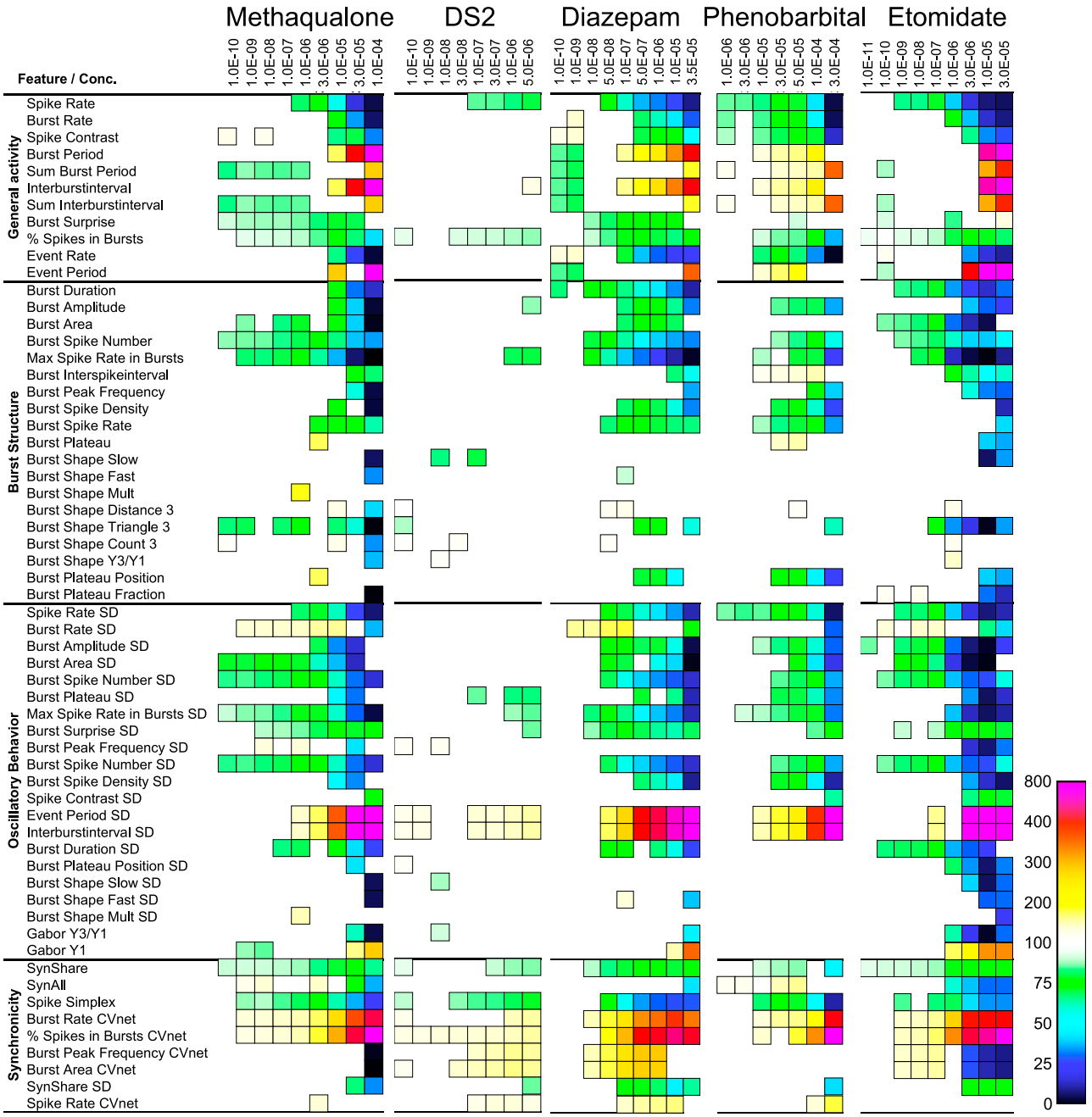

Fig. 8. Summary of the changes induced by methaqualone, DS2, diazepam, phenobarbital, and etomidate on cortical network activity in vitro. The heat maps present the significant changes in 60 activity-describing parameters from four defined categories arising from eight or nine cumulatively increasing concentrations of the five modulators (concentrations are given in molar). The colors encode statistically significant modulator-induced changes (increases or decreases) in parameters relative to native activity (no drug, 100%).

Concentration-Effect Relationships for Methaqualone and Other $GABA_AR$ Modulators in the Network Recordings. The overall profile of methaqualone in the recordings reflected in the 60 best-describing parameters was quite characteristic for a CNS depressant (Figs. 8 and 9). Application of the modulator in concentrations found to elicit significant effects at the recombinant $GABA_ARs$ in the TEVC recordings (1–100 μM) resulted in significantly reduced spike and burst rates and increased the interval between bursts as well as the average burst period. Moreover, burst sizes were significantly reduced by the presence of these methaqualone concentrations (e.g., decreases in burst duration, burst area, and burst amplitude) (Figs. 8 and 9). The decreased variability observed for several of the burst structure parameters (e.g., burst area S.D. and burst spike number S.D.) indicated a more regular burst structure, whereas the overall bursting activity was observed to be more irregular (increase in burst rate S.D., interburst interval S.D., event period S.D.). Finally, increased network variability (e.g., burst rate CVnet and other CVnet parameters, decreased SynShare, the average number of units involved in population bursts) indicative of decreased synchronization within the network

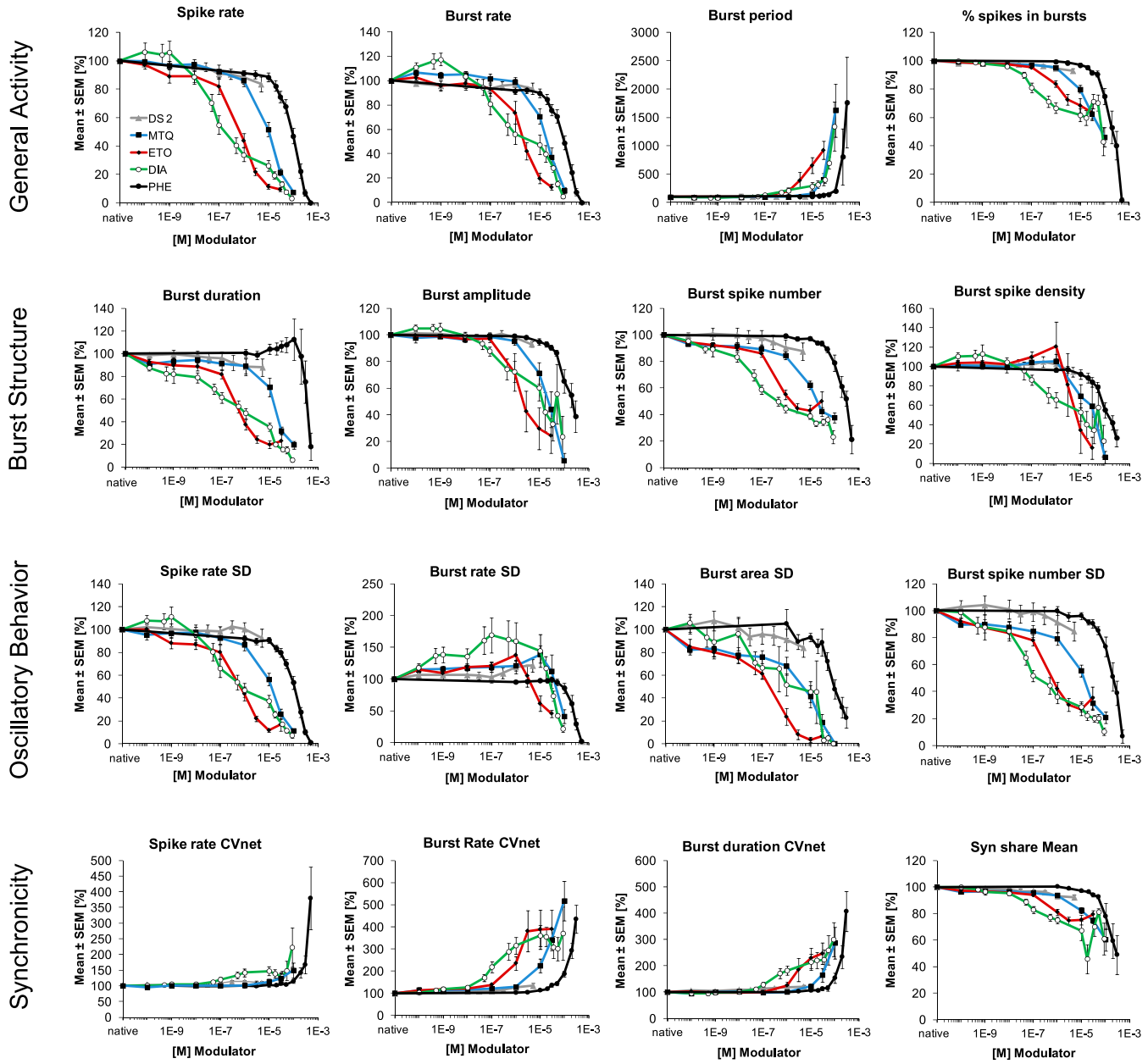

Fig. 9. Selected functional effects of methaqualone, DS2, etomidate, phenobarbital, and diazepam on cortical network activity in vitro. The effects of eight or nine cumulatively increasing concentrations of methaqualone (black square, blue line), DS2 (gray triangle, gray line), phenobarbital (black circle, black line), diazepam (open circle, green line), and etomidate (black diamond, red line) at 16 activity-describing parameters from four defined categories. Data are given as mean ± S.E.M. relative to native activity (no drug, 100%).

was observed at these modulator concentrations (Figs. 8 and 9). Interestingly, submicromolar concentrations of methaqualone also mediated significant effects on network activity although these were very subtle (Figs. 8 and 9).

The functional characteristics of methaqualone in the MEA recordings were compared with those exhibited by four other GABA$_A$R modulators: the benzodiazepine diazepam, the barbiturate phenobarbital, the general anesthetic etomidate, and DS2, a selective PAM of δ-containing GABA$_A$Rs (Wafford et al., 2009). The multiparametric effects mediated by diazepam, etomidate, and phenobarbital at the cortical networks were quite similar to those induced by methaqualone, the different concentration-response relationships displayed by the four modulators being easily reconcilable with their different potencies as a GABA$_A$R PAMs (Figs. 8 and 9). However, while the qualitatively trend in the changes induced by methaqualone, diazepam, etomidate, and phenobarbital was the same for most parameters, some interesting differences were observed. For example, high or saturating concentrations of etomidate or methaqualone induced more pronounced changes in some of the "General Activity", "Burst Structure", and "Oscillatory Behavior" parameters than high or saturating concentrations of phenobarbital or diazepam (Fig. 8). The general effects of DS2 on cortical network activity were much more subtle than those produced by the four other modulators, but most of the changes induced by this PAM were characterized by the same qualitative directions of parameter changes (Figs. 8 and 9).

Similarity Analysis and Classification. To assess the extent to which the effects of methaqualone at neuronal network activity resembled those induced by other types of CNS drugs and neuroactive compounds and whether its in vivo properties potentially could be ascribed to additional activity components than its $GABA_AR$ activity, the "phenotypic fingerprint" of the drug was compared with those exhibited by 69 reference compounds. This similarity analysis compares characteristics and patterns of the effects induced by the respective drugs on the activity-describing recording parameters, which means that compounds exhibiting different degrees of effects on a parameter can be classified as similar. The database compounds selected for the analysis in the present study comprised compounds targeting numerous different neurotransmitter systems through various mechanisms and included several classes of clinically administered therapeutics, including antidepressants, antipsychotics, anticonvulsants, antisedatives, analgesics, anesthetics, and procognitive drugs (Table 3). A training data set with the 204 spike train parameters was established using the data records for the 69 reference compounds, and subsequently the data records of methaqualone were classified as previously described (Parenti et al., 2013), resulting in a ranking list reflecting the functional similarity of each of the methaqualone concentrations with the database compounds. Thus, the effects mediated by specific methaqualone concentrations were compared with the profiles of each of the reference compounds (i.e., the averaged effects induced by multiple concentrations of the reference compound). With the exception of the classic antipsychotic drug chlorpromazine and the antidepressant amitriptyline, the database compounds giving rise to effects exhibiting the highest similarities to those mediated by methaqualone (1–100 μM) were $GABA_AR$ PAMs (etomidate, diazepam, thiopental, clonazepam), NMDA receptor antagonists (MK801 [(5*S*,10*R*)-(+)-5-methyl-10,11-dihydro-5*H*-dibenzo[*a,d*]cyclohepten-5,10-imine maleate], memantine), and other CNS depressants (valproate, retigabine) (Fig. 10).

TABLE 3
The 69 NeuroProof database compounds compared with methaqualone in the similarity analysis

Acetaminophen	Epibatidine	Muscimol
Agmatine	Eserine	Olanzapine
Amisulpride	Etomidate	Oxotremorine
Amitriptyline	Flumazenil	Pentylenetetrazolium
AMPA	Flunitrazepam	Phenytoin
Apomorphine	Fluoxetine	Picrotoxin
Aripiprazole	GABA	Propofol
Atropine	Galanthamine	Quetiapine
Baclofen	GS 39783	Retigabine
Benzoquinone	Haloperidol	Risperidone
Carbamazepine	Ibuprofen	SB 205384
CGP 7930	Indatraline	SCH 50911
Chlorpromazine	L-655708	SKF-97541
CL218872	L-838417	Sufentanil
Clobazam	Lamotrigine	Thiopental
Clonazepam	Levetiracetam	Thio-THIP
Clozapine	L-Polamidon	THIP
"Control"	LY341495	Topiramate
D-Cycloserine	LY354740	Tramadol
Diazepam	LY393558	Valproate
Dimethylsulfoxide	Memantine	Wortmannin
Donepezil	MK801	Xli093
DS2	Morphine	Zolpidem

CGP 7930, 2,6-ditert-butyl-4-(3-hydroxy-2,2-dimethylpropyl)phenol; CL218872, 3-methyl-6-[-3-(trifluoromethyl)phenyl]-1,2,4-triazolo[4,3-*b*]pyridazine; GS 39783, 4-*N*,6-*N*-dicyclopentyl-2-methylsulfanyl-5-nitropyrimidine-4,6-diamine; L-655708, ethyl (*S*)-11,12,13,13*a*-tetrahydro-7-methoxy-9-oxo-9*H*-imidazo[1,5-*a*]pyrrolo[2,1-*c*][1,4]benzodiazepine-1-carboxylate; L-838417, 7-tert-butyl-3-(2,5-difluorophenyl)-6-[(2-methyl-1,2,4-triazol-3-yl)methoxy]-[1,2,4]triazolo[4,3-b]pyridazine; LY341495, (1*S*,2*S*)-2-[(1*S*)-1-amino-1-carboxy-2-(9*H*-xanthen-9-yl)ethyl]cyclopropane-1-carboxylic acid; LY354740, (1*S*,2*S*,5*R*,6*S*)-2-aminobicyclo[3.1.0]hexane-2,6-dicarboxylic acid; LY393558, 1-[2-[4-(6-fluoro-1*H*-indol-3-yl)-3,6-dihydro-1(2*H*)-pyridinyl]ethyl]-3,4-dihydro-3-(1-methylethyl)-6-(methylsulfonyl)-1*H*-2,1,3-benzothiadiazine-2,2-dioxide; SB 205384, but-2-ynyl 4-amino-7-hydroxy-2-methyl-5,6,7,8-tetrahydro-[1]benzothiolo[2,3-*b*]pyridine-3-carboxylate; SCH 50911, (2*S*)-(+)-5,5-dimethyl-2-morpholineacetic acid; SKF-97541, 3-aminopropyl(methyl)phosphinic acid; THIP, 4,5,6,7-tetrahydroisoxazolo[5,4-*c*]pyridin-3-ol; Xli093, bis[8-ethynyl-5,6-dihydro-5-methyl-6-oxo-4*H*-imidazo[1,5-*a*][1,4]benzodiazepine-3-carboxylic acid] 1,3-propanediyl ester hydrate.

In Vivo Exposure and Efficacy of Methaqualone in Seizure Threshold and Motor Coordination Assays

To investigate to what extent the in vitro properties displayed by methaqualone at $GABA_ARs$ correlated with its in vivo efficacy, exposure studies of the drug were combined with testing it in MEST and beam-walk assays in mice using diazepam as a reference $GABA_AR$ modulator (Fig. 11).

In preliminary exposure studies, plasma and brain concentrations of methaqualone were determined 15, 30, 60, and 120 minutes after subcutaneous administration of 10 mg/kg of the drug, and since both concentrations peaked at 60 minutes, this study design was used for the subsequent experiments. After administration of 10-, 30-, and 100-mg/kg doses of methaqualone, plasma concentrations of the drug were determined to 2.79 ± 0.57, 12.3 ± 0.93, and 26.7 ± 0.63 μg/ml, respectively, and brain concentrations to 0.71 ± 0.10, 4.1 ± 0.23, and 16.1 ± 0.27 μg/g, respectively (means ± S.E.M.; n = 3). Since the levels of free (unbound) fraction of methaqualone in mouse brain homogenates were determined to be 13%, corresponding unbound concentrations of methaqualone in brain were estimated at 0.37 ± 0.05, 2.14 ± 0.12, and 8.38 ± 0.14 μM for the 10-, 30-, and 100-mg/kg doses, respectively (Fig. 11A). Plasma and brain concentrations of the reference drug diazepam were not determined in this study; however, a previous study has found subcutaneous administration of 3 mg/kg of diazepam in mice to produce a total brain concentration of 400 ng/g (30 minutes after administration) (Doran et al., 2005), and we have determined the fraction of free (unbound) diazepam in mouse brain to be 3%. Extrapolating from this finding, the 0.3-, 1-, and 3-mg/kg diazepam doses used in this study (Fig. 11B) would correspond to brain free diazepam concentrations of approximately 4, 15, and 40 nM, respectively.

Both methaqualone and diazepam displayed significant effects in the two animal models. Whereas subcutaneous administration of 100 mg/kg of methaqualone significantly increased seizure threshold in the animals in the MEST assay, administration of 30 or 100 mg/kg of methaqualone resulted in significantly increased numbers of slips and falls in the beam-walk assay (Fig. 11A). Analogously, diazepam and other benzodiazepines in these models induced significant sedative or ataxia effects at lower doses than those required to produce significant anticonvulsant effects (Fig. 11B and unpublished data). The doses of the two drugs needed to induce sedative or ataxia and anticonvulsant effects could seem somewhat high at first glance. However, it is well documented that behavioral readouts in rodents and humans on drug treatment do not always correlate, something that has been ascribed to the substantially faster hepatic clearance

	Methaqualone [M]	1.E-09	1.E-08	1.E-07	1.E-06	3.E-06	1.E-05	3.E-05	1.E-04	mean %
1	Etomidate (1E-11 - 3E-05 M)	2%	3%	4%	7%	6%	6%	6%	8%	7%
2	Diazepam (1E-10 - 9E-05 M)	0%	1%	1%	4%	8%	9%	6%	4%	6%
3	Chlorpromazine (1E-9 - 0.9E-03 M)	0%	0%	0%	0%	0%	2%	13%	12%	5%
4	MK801 (1E-10 - 5E-05 M)	0%	0%	0%	0%	0%	4%	10%	11%	5%
5	Thiopental (1E-8 - 2E-05 M)	3%	3%	2%	5%	7%	8%	2%	1%	5%
6	Memantine (1E-14 - 1E-04 M)	0%	1%	0%	2%	2%	6%	7%	5%	4%
7	Valproate (1E-07 - 2E-02 M)	1%	2%	2%	5%	3%	1%	2%	7%	4%
8	Amitriptyline (1E-12 - 1E-03 M)	5%	3%	5%	5%	3%	0%	4%	4%	3%
9	Retigabine (1E-10 - 1E-04 M)	7%	5%	6%	6%	4%	2%	0%	4%	3%
10	Clonazepam (1E-11 - 1E-04 M)	0%	0%	0%	0%	0%	4%	6%	3%	3%
69	Baclofen	0%	0%	0%	0%	0%	0%	0%	0%	0%
	sum	100%	100%	100%	100%	100%	100%	100%	100%	100%

Fig. 10. Similarity analysis of the effects of methaqualone at cortical network activity. Top 10 ranks of the most phenotypically similar functional profiles of 69 reference compounds from the NeuroProof database (listed in Table 3) ranked based on the similarity score for methaqualone at concentrations ranging from 1 to 100 μM. Data for the methaqualone concentrations 1, 10, and 100 nM are given in shaded colors. The concentration-response profiles of the 69 reference compounds were used for training the classifier, and the methaqualone data sets were classified per concentration (10 per concentration). Table values correspond to similarity score per concentration (e.g., at 100 μM methaqualone, 8% of its data sets were classified as etomidate, 4% as diazepam, 12% as chlorpromazine, and so forth). High values reflect high functional phenotypic similarity between reference compound effects and methaqualone effects.

and drug metabolism in rodents (Lave et al., 1999; Sharma and McNeill, 2009).

Discussion

Investigations into the mechanisms of action of old CNS drugs hold interesting perspectives. Although a drug may have been shelved for good reasons, new insights into the molecular basis for its clinical efficacy can open new avenues of drug development, as exemplified by the current interest in ketamine as a lead for novel antidepressants (Sanacora and Schatzberg, 2015). Moreover, these explorations can shed light on previous observations for the drug and its target and could potentially reinvent the drug as a useful pharmacologic tool. In the present study, the notorious past and elusive mode of action of methaqualone (and other quaaludes) prompted us to explore the molecular basis underlying its therapeutic and recreational effects.

Methaqualone Is a Multifaceted $GABA_AR$ Modulator. Methaqualone was found to be a pan-active $GABA_AR$ modulator exhibiting activity at 12 of 13 $GABA_AR$ subtypes (Table 1). Albeit a relatively pure PAM at most of these receptors, methaqualone exhibited everything from inactivity over negative or positive modulation to pronounced agonism within this selection of subtypes. Moreover, the nature of its potentiation of $\alpha_{1,2,3,5}\beta_{2,3}\gamma_{2S}$ and $\alpha_4\beta_2\delta/\alpha_6\beta_{2,3}\delta$ signaling differed, as it exclusively modulated GABA potency at the $\alpha\beta\gamma$ receptor, whereas it increased both GABA potency and efficacy at the $\alpha\beta\delta$ receptor. The presence of γ_2 or δ in the $GABA_AR$ was clearly not a prerequisite for methaqualone-mediated modulation, but these differential PAM characteristics nevertheless must be ascribed to the distinct functional properties of $\alpha\beta\gamma$ and $\alpha\beta\delta$ receptors. Whereas the remarkable high-efficacious direct activation of the $\alpha_4\beta_3\delta$ receptor mediated by methaqualone could be a reflection of true allosteric agonism, we cannot exclude that it could arise from potentiation of the pronounced spontaneous activity of this receptor, analogously to the mechanism proposed to underlie the apparent agonism displayed by DS2 at this receptor in a recent study (Jensen et al., 2013). The fact that etomidate also displays superagonism at $\alpha_4\beta_3\delta$ seems to support this latter hypothesis (Fig. 5). Conversely, the inability of both modulators to potentiate the constitutive activity exhibited by the $\alpha_4\beta_1\delta$ receptor suggests that they could possess true intrinsic agonist activity at $\alpha_4\beta_3\delta$ or, alternatively, that the molecular basis for the spontaneous activity of $\alpha_4\beta_1\delta$ may differ from that of $\alpha_4\beta_3\delta$ (Fig. 5).

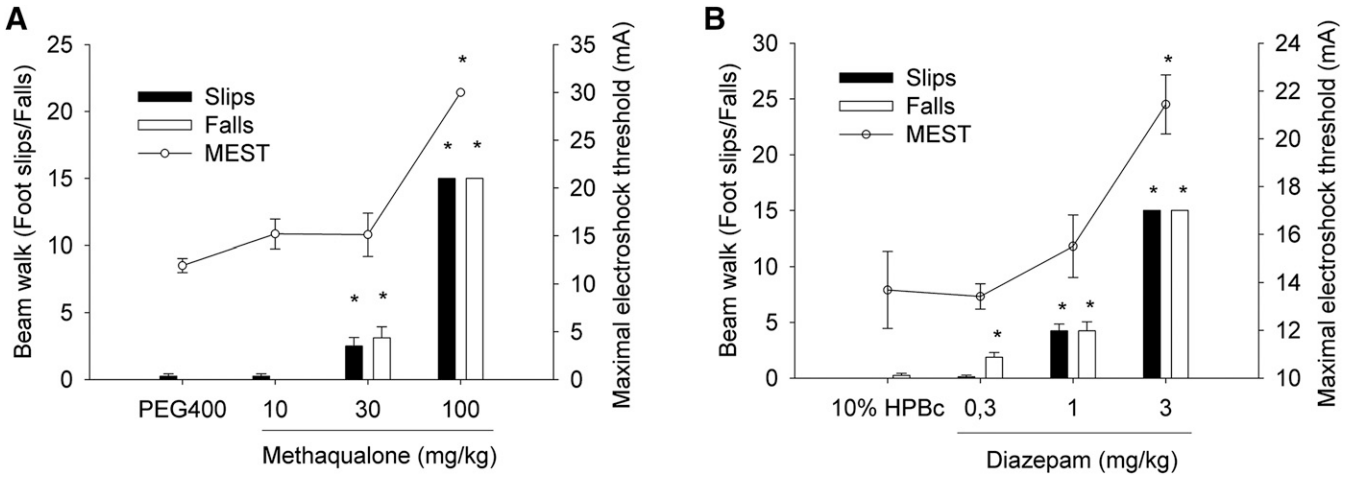

Fig. 11. Sedative or ataxic effects and anticonvulsant efficacy of methaqualone (A) and diazepam (B) in beam walk and MEST assays in mice. Data are given as average slips and falls (mean ± S.E.M.) and by the average current threshold (mean ± S.E.M.), respectively. *$P < 0.05$ analysis of variance and post hoc Dunnett's test. HPBc; hydroxypropyl-β-cyclodextrin

The comparable functional potencies displayed by methaqualone as PAM, NAM, or agonist at the various $GABA_ARs$ suggest that the modulator targets a uniform binding site in the receptors, a hypothesis further supported by the complete reversal of its modulatory properties at the $\alpha_6\beta_1\delta$ and $\alpha_6\beta_2\delta$ receptors brought on by β_1-S265N and β_2-N265S mutations (Fig. 4, B and C). Thus, the diverse functionalities of methaqualone are more likely to arise from different energy barriers underlying allosteric transitions in the respective subtypes than from the modulator targeting different sites or having substantially different binding modes in the receptors. Although the inactivity of methaqualone at $\alpha_4\beta_1\delta$ would constitute an outlier in this scenario if rooted in low binding affinity, the compound could also be envisioned to act as a neutral ligand (or silent allosteric modulator) at this subtype. We will refrain from further speculations about this, however, not having investigated the basis for the lack of modulation at this subtype. Analogously to the notion of methaqualone exerting its multifaceted pharmacology through a uniform site in the $GABA_ARs$, some benzodiazepine-site ligands display functional selectivity at $\alpha_{1,2,3,5}\beta\gamma_2$ receptors (Dawson et al., 2006; de Lucas et al., 2015), and allosteric modulators of other receptor types have also been shown to mediate subtype-specific modulation (Mathiesen et al., 2003; Marlo et al., 2009; Costa et al., 2010).

The bell-shaped concentration-response curves and rebound currents obtained for methaqualone at the $GABA_ARs$ are very similar to those observed for other PAMs/ago-PAMs acting through the transmembrane receptor domains (Fig. 1, C and D) (Hill-Venning et al., 1997; Wooltorton et al., 1997; Halliwell et al., 1999; Feng and Macdonald, 2004; Feng et al., 2004; Khom et al., 2007). In several of these cases, the submaximal potentiation observed at high modulator concentrations has been attributed to the existence of a low-affinity open-channel block site, with the rebound currents arising from the rapid unbinding of the modulator from this site (Wooltorton et al., 1997; Halliwell et al., 1999; Feng et al., 2004; Khom et al., 2007). This also seems a plausible explanation for methaqualone, although the submaximal potentiation at high modulator concentrations also could be caused by increased receptor desensitization.

The Methaqualone Binding Site. Solid experimental evidence indicates that methaqualone does not act through the benzodiazepine, barbiturate, or neurosteroid binding sites in the $GABA_AR$ (Fig. 3). We propose that the key importance of β-subunit identity and of β-residue 265 for the functionality of methaqualone constitutes a strong case for the transmembrane $\beta^{(+)}/\alpha^{(-)}$ interface as the targeted receptor region. In contrast, there are compelling reasons to be cautious when speculating about the exact location of the binding site within this interface. Allosteric modulators bind quite differently to the transmembrane subunit interfaces in Cys-loop receptors (Hibbs and Gouaux, 2011; Trattnig et al., 2012; Sauguet et al., 2013; Stewart et al., 2013; Lansdell et al., 2015) and having only investigated two residues as putative binding partners, we can hardly claim to have obtained a detailed insight into the binding mode of methaqulone. Albeit the changed modulation displayed by methaqualone at $\alpha_1{}^{M236W}\beta_2\gamma_{2S}$ and $\alpha_1\beta_2{}^{M286W}\gamma_{2S}$ receptors could indicate involvement of these residues in modulator binding, it could also arise from allosteric effects of the introduced mutations (Siegwart et al., 2002; Chiara et al., 2012). However, the structural similarities between methaqualone, etomidate, and loreclezole and the common pharmacophore identified for them support the notion of a shared binding site (Fig. 6), analogously to what has been proposed for etomidate, loreclezole, and mefenamic acid (Halliwell et al., 1999). Thus, these "β-residue 265 sensitive" modulators could be envisioned to act through such a common site, with ligands not sensitive to changes in this position possibly binding differently to this interface (Thompson et al., 2004).

Functional Characteristics of Methaqualone at Cortical Neurons. All in all, the effects of methaqualone on neuronal firing patterns in cortical networks seem to be reconcilable with its $GABA_AR$ activity, and comparison of these effects to those induced by other $GABA_AR$ modulators serves to elucidate the contributions from the different activity components of the modulator (Figs. 8 and 9). The four modulators targeting $\alpha\beta\gamma$ receptors (methaqualone, diazepam, etomidate, and phenobarbital) all induced pronounced changes in the spontaneous activity patterns, and thus augmentation of synaptic $GABA_AR$ signaling appears to be key for overall effects on cortical network activity. In contrast, the much more subtle effects induced by DS2 indicate that the isolated contributions from the potentiation of δ-containing $GABA_ARs$ to network activity are minor. Nevertheless, this activity component could be important for the observed effects of methaqualone since potentiation of these extrasynaptic $GABA_ARs$ would be expected to affect the firing threshold of the neurons.

The key role of $GABA_ARs$ for the methaqualone-mediated effects is further supported by the high-ranking of several $GABA_AR$ PAMs, NMDA receptor antagonists, and other known CNS depressants in the similarity analysis comparing the network activity effects of methaqualone to the phenotypic profiles of 69 reference compounds with diverse pharmacologic and therapeutic properties (Fig. 10; Table 3). The high-ranking of chlorpromazine constitutes a notable exception in this respect. Although micromolar chlorpromazine concentrations have been reported to modulate GABAergic currents in hippocampal neurons (Mozrzymas et al., 1999a,b), it is a highly promiscuous drug with potent activity at numerous receptors, transporters, and ion channels, and thus its effects on neuronal network activity are likely to arise from several other mediators.

Correlation between In Vitro $GABA_AR$ Activity and In Vivo Efficacy of Methaqualone. As discussed above, the negligible activity displayed by methaqualone at a plethora of neurotransmitter targets in the screening and its effects on cortical network activity in the MEA recordings all in all seem to indicate that it is a fairly selective $GABA_AR$ modulator (Figs. 7–10; Table 2). This finding prompted us to investigate whether its $GABA_AR$ activity could account for its in vivo efficacy. The estimated free (unbound) methaqualone concentrations in mouse brain arising from in vivo effective doses (2–8 μM) were in the very low end of the effective concentration range for the modulator at $GABA_ARs$ in the TEVC recordings. This apparent mismatch is unlikely to arise from substantially different pharmacologic properties of methaqualone at recombinant human and native rodent $GABA_ARs$, just as it seems improbable that its in vivo effects are mediated through another target. Instead, it could simply be a reflection of allosteric $GABA_AR$ modulators being efficacious in vivo at low levels of receptor occupancy.

Interestingly, the estimated free concentrations of diazepam in mice brains produced by in vivo effective doses (4–40 nM) were also substantially lower than the functional potency of the benzodiazepine at recombinant $\alpha\beta\gamma$ $GABA_ARs$ (EC_{50} ~100 nM). In this light, our data could support the notion of $GABA_ARs$ as the key mediators of the in vivo effects of methaqualone.

Conclusion. The present delineation of the molecular basis for the behavioral effects of methaqualone does more than confirm what has been assumed for decades: that the drug mediates these effects through $GABA_ARs$. Methaqualone exhibits distinct functional properties at the $GABA_ARs$ compared with other allosteric modulators, and it mediates these through a different mechanism than the barbiturates and benzodiazepines that it historically has been lumped together with. It is tempting to speculate that these differences could contribute to the reported differences in the in vivo effects induced by methaqualone and classic CNS depressants. In any case, the multifaceted functionality of methaqualone at $GABA_ARs$ seems to be at the root of its clinical efficacy, as well as the addiction liability and recreational misuse associated with the drug.

Acknowledgments

The authors thank Dr. P. J. Whiting and Merck, Sharpe, and Dohme Research Laboratories for the generous gifts of the human $GABA_AR$ cDNAs, and Dr. S. Mennerick for kind advice.

Authorship Contributions

Participated in research design: Hammer, Bader, Schroeder, Bastlund, Gramowski-Voß, Jensen.

Conducted experiments: Hammer, Bader, Ehnert, Bundgaard, Bunch, Jensen.

Performed data analysis: Hammer, Bader, Ehnert, Hoestgaard-Jensen, Bastlund, Jensen.

Wrote or contributed to the writing of the manuscript: Hammer, Bader, Jensen (with contributions from Ehnert, Bundgaard, Bunch, Bastlund).

References

Bali M and Akabas MH (2004) Defining the propofol binding site location on the $GABA_A$ receptor. *Mol Pharmacol* **65**:68–76.

Barcelo R (1961) A clinical study of methaqualone: a new nonbarbiturate hypnotic. *Can Med Assoc J* **85**:1304–1305.

Barceloux DG (2012) Methaqualone and related compounds, in Medical Toxicology of Drug Abuse, pp 504–513, John Wiley & Sons, Inc., New York.

Belelli D, Harrison NL, Maguire J, Macdonald RL, Walker MC, and Cope DW (2009) Extrasynaptic $GABA_A$ receptors: form, pharmacology, and function. *J Neurosci* **29**: 12757–12763.

Belelli D, Lambert JJ, Peters JA, Wafford K, and Whiting PJ (1997) The interaction of the general anesthetic etomidate with the γ-aminobutyric acid type A receptor is influenced by a single amino acid. *Proc Natl Acad Sci USA* **94**:11031–11036.

Brickley SG and Mody I (2012) Extrasynaptic $GABA_A$ receptors: their function in the CNS and implications for disease. *Neuron* **73**:23–34.

Brown N, Kerby J, Bonnert TP, Whiting PJ, and Wafford KA (2002) Pharmacological characterization of a novel cell line expressing human $\alpha_4\beta_3\delta$ $GABA_A$ receptors. *Br J Pharmacol* **136**:965–974.

Campo-Soria C, Chang Y, and Weiss DS (2006) Mechanism of action of benzodiazepines on $GABA_A$ receptors. *Br J Pharmacol* **148**:984–990.

Carroll M and Gallo G (1985) *Quaaludes: The Quest for Oblivion*, Chelsea House, New York.

Chen ZW, Wang C, Krishnan K, Manion BD, Hastings R, Bracamontes J, Taylor A, Eaton MM, Zorumski CF, and Steinbach JH et al. (2014) 11-trifluoromethyl-phenyldiazirinyl neurosteroid analogues: potent general anesthetics and photolabeling reagents for $GABA_A$ receptors. *Psychopharmacology (Berl)* **231**: 3479–3491.

Chiara DC, Dostalova Z, Jayakar SS, Zhou X, Miller KW, and Cohen JB (2012) Mapping general anesthetic binding site(s) in human α1β3 γ-aminobutyric acid type A receptors with [^{3}H]TDBzl-etomidate, a photoreactive etomidate analogue. *Biochemistry* **51**:836–847.

Chiara DC, Jayakar SS, Zhou X, Zhang X, Savechenkov PY, Bruzik KS, Miller KW, and Cohen JB (2013) Specificity of intersubunit general anesthetic-binding sites in the transmembrane domain of the human α1β3γ2 γ-aminobutyric acid type A ($GABA_A$) receptor. *J Biol Chem* **288**:19343–19357.

Costa BM, Irvine MW, Fang G, Eaves RJ, Mayo-Martin MB, Skifter DA, Jane DE, and Monaghan DT (2010) A novel family of negative and positive allosteric modulators of NMDA receptors. *J Pharmacol Exp Ther* **335**:614–621.

Dawson GR, Maubach KA, Collinson N, Cobain M, Everitt BJ, MacLeod AM, Choudhury HI, McDonald LM, Pillai G, and Rycroft W, et al. (2006) An inverse agonist selective for α5 subunit-containing $GABA_A$ receptors enhances cognition. *J Pharmacol Exp Ther* **316**:1335–1345.

de Lucas AG, Ahring PK, Larsen JS, Rivera-Arconada I, Lopez-Garcia JA, Mirza NR, and Munro G (2015) $GABA_A$ α5 subunit-containing receptors do not contribute to reversal of inflammatory-induced spinal sensitization as indicated by the unique selectivity profile of the $GABA_A$ receptor allosteric modulator NS16085. *Biochem Pharmacol* **93**:370–379.

Desai R, Ruesch D, and Forman SA (2009) γ-amino butyric acid type A receptor mutations at β2N265 alter etomidate efficacy while preserving basal and agonist-dependent activity. *Anesthesiology* **111**:774–784.

Doran A, Obach RS, Smith BJ, Hosea NA, Becker S, Callegari E, Chen C, Chen X, Choo E, and Cianfrogna J et al. (2005) The impact of P-glycoprotein on the disposition of drugs targeted for indications of the central nervous system: evaluation using the MDR1A/1B knockout mouse model. *Drug Metab Dispos* **33**:165–174.

Falco M (1976) Methaqualone misuse: foreign experience and United States drug control policy. *Int J Addict* **11**:597–610.

Feng HJ, Bianchi MT, and Macdonald RL (2004) Pentobarbital differentially modulates α1β3δ and α1β3γ2L $GABA_A$ receptor currents. *Mol Pharmacol* **66**:988–1003.

Feng HJ and Macdonald RL (2004) Multiple actions of propofol on αβγ and αβδ $GABA_A$ receptors. *Mol Pharmacol* **66**:1517–1524.

Feng HJ and Macdonald RL (2010) Barbiturates require the N terminus and first transmembrane domain of the δ subunit for enhancement of α1β3δ $GABA_A$ receptor currents. *J Biol Chem* **285**:23614–23621.

Gass JT (2008) *Drugs The Straight Facts: Qualuudes*, Chelsea House, New York.

Ghiani CA, Tuligi G, Maciocco E, Serra M, Sanna E, and Biggio G (1996) Biochemical evaluations of the effects of loreclezole and propofol on the $GABA_A$ receptor in rat brain. *Biochem Pharmacol* **51**:1527–1534.

Gielen MC, Lumb MJ, and Smart TG (2012) Benzodiazepines modulate $GABA_A$ receptors by regulating the preactivation step after GABA binding. *J Neurosci* **32**: 5707–5715.

Gramowski A, Jügelt K, Stüwe S, Schulze R, McGregor GP, Wartenberg-Demand A, Loock J, Schröder O, and Weiss DG (2006a) Functional screening of traditional antidepressants with primary cortical neuronal networks grown on multielectrode neurochips. *Eur J Neurosci* **24**:455–465.

Gramowski A, Jügelt K, Weiss DG, and Gross GW (2004) Substance identification by quantitative characterization of oscillatory activity in murine spinal cord networks on microelectrode arrays. *Eur J Neurosci* **19**:2815–2825.

Gramowski A, Stüwe S, Jügelt K, Schiffmann D, Loock J, Schröder O, Gross GW, and Weiss DG (2006b) Detecting neurotoxicity through electrical activity changes of neuronal networks on multielectrode neurochips. *ALTEX* **23**:410–415.

Green AR, Misra A, Murray TK, Snape MF, and Cross AJ (1996) A behavioural and neurochemical study in rats of the pharmacology of loreclezole, a novel allosteric modulator of the $GABA_A$ receptor. *Neuropharmacology* **35**:1243–1250.

Greenfield LJ, Jr, Zaman SH, Sutherland ML, Lummis SC, Niemeyer MI, Barnard EA, and Macdonald RL (2002) Mutation of the $GABA_A$ receptor M1 transmembrane proline increases GABA affinity and reduces barbiturate enhancement. *Neuropharmacology* **42**:502–521.

Halliwell RF, Thomas P, Patten D, James CH, Martinez-Torres A, Miledi R, and Smart TG (1999) Subunit-selective modulation of $GABA_A$ receptors by the non-steroidal anti-inflammatory agent, mefenamic acid. *Eur J Neurosci* **11**:2897–2905.

Herd MB, Belelli D, and Lambert JJ (2007) Neurosteroid modulation of synaptic and extrasynaptic $GABA_A$ receptors. *Pharmacol Ther* **116**:20–34.

Herzberg D (2011) Blockbusters and controlled substances: Miltown, Quaalude, and consumer demand for drugs in postwar America. *Stud Hist Philos Biol Biomed Sci* **42**:415–426.

Hibbs RE and Gouaux E (2011) Principles of activation and permeation in an anion-selective Cys-loop receptor. *Nature* **474**:54–60.

Hicks TP, Kaneko T, and Oka JI (1990) Receptive-field size of S1 cortical neurones is altered by methaqualone via a GABA mechanism. *Can J Neurol Sci* **17**:30–34.

Hill-Venning C, Belelli D, Peters JA, and Lambert JJ (1997) Subunit-dependent interaction of the general anaesthetic etomidate with the γ-aminobutyric acid type A receptor. *Br J Pharmacol* **120**:749–756.

Hoestgaard-Jensen K, Dalby NO, Krall J, Hammer H, Krogsgaard-Larsen P, Frølund B, and Jensen AA (2014) Probing α4βδ $GABA_A$ receptor heterogeneity: differential regional effects of a functionally selective α4β1δ/α4β3δ receptor agonist on tonic and phasic inhibition in rat brain. *J Neurosci* **34**:16256–16272.

Hoestgaard-Jensen K, O'Connor RM, Dalby NO, Simonsen C, Finger BC, Golubeva A, Hammer H, Bergmann ML, Kristiansen U, and Krogsgaard-Larsen P et al. (2013) The orthosteric $GABA_A$ receptor ligand Thio-4-PIOL displays distinctly different functional properties at synaptic and extrasynaptic receptors. *Br J Pharmacol* **170**:919–932.

Hosie AM, Clarke L, da Silva H, and Smart TG (2009) Conserved site for neurosteroid modulation of $GABA_A$ receptors. *Neuropharmacology* **56**:149–154.

Hosie AM, Wilkins ME, da Silva HM, and Smart TG (2006) Endogenous neurosteroids regulate $GABA_A$ receptors through two discrete transmembrane sites. *Nature* **444**:486–489.

Ionescu-Pioggia M, Bird M, Orzack MH, Benes F, Beake B, and Cole JO (1988) Methaqualone. *Int Clin Psychopharmacol* **3**:97–109.

Jensen AA, Bergmann ML, Sander T, and Balle T (2010) Ginkgolide X is a potent antagonist of anionic Cys-loop receptors with a unique selectivity profile at glycine receptors. *J Biol Chem* **285**:10141–10153.

Jensen ML, Wafford KA, Brown AR, Belelli D, Lambert JJ, and Mirza NR (2013) A study of subunit selectivity, mechanism and site of action of the δ selective compound 2 (DS2) at human recombinant and rodent native $GABA_A$ receptors. *Br J Pharmacol* **168**:1118–1132.

Johnstone AF, Gross GW, Weiss DG, Schroeder OH, Gramowski A, and Shafer TJ (2010) Microelectrode arrays: a physiologically based neurotoxicity testing platform for the 21st century. *Neurotoxicology* **31**:331–350.

Karim N, Wellendorph P, Absalom N, Bang LH, Jensen ML, Hansen MM, Lee HJ, Johnston GA, Hanrahan JR, and Chebib M (2012) Low nanomolar GABA effects at extrasynaptic $\alpha4\beta1/\beta3\delta$ $GABA_A$ receptor subtypes indicate a different binding mode for GABA at these receptors. *Biochem Pharmacol* **84**:549–557.

Karim N, Wellendorph P, Absalom N, Johnston GA, Hanrahan JR, and Chebib M (2013) Potency of GABA at human recombinant $GABA_A$ receptors expressed in Xenopus oocytes: a mini review. *Amino Acids* **44**:1139–1149.

Keov P, Sexton PM, and Christopoulos A (2011) Allosteric modulation of G protein-coupled receptors: a pharmacological perspective. *Neuropharmacology* **60**:24–35.

Khom S, Baburin I, Timin E, Hohaus A, Trauner G, Kopp B, and Hering S (2007) Valerenic acid potentiates and inhibits $GABA_A$ receptors: molecular mechanism and subunit specificity. *Neuropharmacology* **53**:178–187.

Kimball AW, Burnett WT, Jr, and Doherty DG (1957) Chemical protection against ionizing radiation. I. Sampling methods for screening compounds in radiation protection studies with mice. *Radiat Res* **7**:1–12.

Krasowski MD, Nishikawa K, Nikolaeva N, Lin A, and Harrison NL (2001) Methionine 286 in transmembrane domain 3 of the $GABA_A$ receptor β subunit controls a binding cavity for propofol and other alkylphenol general anesthetics. *Neuropharmacology* **41**:952–964.

Lansdell SJ, Sathyaprakash C, Doward A, and Millar NS (2015) Activation of human 5-hydroxytryptamine type 3 receptors via an allosteric transmembrane site. *Mol Pharmacol* **87**:87–95.

Lavé T, Coassolo P, and Reigner B (1999) Prediction of hepatic metabolic clearance based on interspecies allometric scaling techniques and in vitro-in vivo correlations. *Clin Pharmacokinet* **36**:211–231.

Li GD, Chiara DC, Sawyer GW, Husain SS, Olsen RW, and Cohen JB (2006) Identification of a $GABA_A$ receptor anesthetic binding site at subunit interfaces by photolabeling with an etomidate analog. *J Neurosci* **26**:11599–11605.

Löscher W and Schmidt D (1988) Which animal models should be used in the search for new antiepileptic drugs? A proposal based on experimental and clinical considerations. *Epilepsy Res* **2**:145–181.

Marlo JE, Niswender CM, Days EL, Bridges TM, Xiang Y, Rodriguez AL, Shirey JK, Brady AE, Nalywajko T, and Luo Q et al. (2009) Discovery and characterization of novel allosteric potentiators of M1 muscarinic receptors reveals multiple modes of activity. *Mol Pharmacol* **75**:577–588.

Mathiesen JM, Svendsen N, Bräuner-Osborne H, Thomsen C, and Ramirez MT (2003) Positive allosteric modulation of the human metabotropic glutamate receptor 4 (hmGluR4) by SIB-1893 and MPEP. *Br J Pharmacol* **138**:1026–1030.

McCarthy G, Myers B, and Siegfried N (2005) Treatment for methaqualone dependence in adults. *Cochrane Database Syst Rev* (2):CD004146.

Meera P, Olsen RW, Otis TS, and Wallner M (2009) Etomidate, propofol and the neurosteroid THDOC increase the GABA efficacy of recombinant $\alpha4\beta3\delta$ and $\alpha4\beta3$ $GABA_A$ receptors expressed in HEK cells. *Neuropharmacology* **56**:155–160.

Mortensen M, Patel B, and Smart TG (2011) GABA potency at $GABA_A$ receptors found in synaptic and extrasynaptic zones. *Front Cell Neurosci* **6**:1–10.

Mozrzymas JW, Barberis A, and Cherubini E (1999a) Facilitation of miniature GABAergic currents by chlorpromazine in cultured rat hippocampal cells. *Neuroreport* **10**:2251–2254.

Mozrzymas JW, Barberis A, Michalak K, and Cherubini E (1999b) Chlorpromazine inhibits miniature GABAergic currents by reducing the binding and by increasing the unbinding rate of $GABA_A$ receptors. *J Neurosci* **19**:2474–2488.

Müller WE, Schläfer U, and Wollert U (1978) Benzodiazepine receptor binding: the interactions of some non-benzodiazepine drugs with specific [^{3}H] diazepam binding to rat brain synaptosomal membranes. *Naunyn Schmiedebergs Arch Pharmacol* **305**:23–26.

Naik SR, Naid PR, and Sheth UK (1978) Involvement of γ-amino butyric acid (GABA) in the anticonvulsant action of methaqualone. *Psychopharmacology (Berl)* **57**: 103–107.

Novellino A, Scelfo B, Palosaari T, Price A, Sobanski T, Shafer TJ, Johnstone AF, Gross GW, Gramowski A, and Schroeder O et al. (2011) Development of microelectrode array based tests for neurotoxicity: assessment of interlaboratory reproducibility with neuroactive chemicals. *Front Neuroeng* **4**:4.

Olsen RW and Sieghart W (2008) International Union of Pharmacology. LXX. Subtypes of γ-aminobutyric $acid_A$ receptors: classification on the basis of subunit composition, pharmacology, and function. Update. *Pharmacol Rev* **60**:243–260.

Parenti C, Turnaturi R, Aricò G, Gramowski-Voss A, Schroeder OH, Marrazzo A, Prezzavento O, Ronsisvalle S, Scoto GM, and Ronsisvalle G et al. (2013) The multitarget opioid ligand LP1's effects in persistent pain and in primary cell neuronal cultures. *Neuropharmacology* **71**:70–82.

Parry CD, Myers B, Morojele NK, Flisher AJ, Bhana A, Donson H, and Plüddemann A (2004) Trends in adolescent alcohol and other drug use: findings from three sentinel sites in South Africa (1997-2001). *J Adolesc* **27**:429–440.

Pfeiffer CC, Goldstein L, and Murphree HB (1968) Quantitative analysis of the effect of methqualone on the human EEG. *J Clin Pharmacol J New Drugs* **8**:235–244.

Quast U and Brenner O (1983) Modulation of [^{3}H]muscimol binding in rat cerebellar and cerebral cortical membranes by picrotoxin, pentobarbitone, and etomidate. *J Neurochem* **41**:418–425.

Redrobe JP, Elster L, Frederiksen K, Bundgaard C, de Jong IE, Smith GP, Bruun AT, Larsen PH, and Didriksen M (2012) Negative modulation of $GABA_A$ $\alpha5$ receptors by RO4938581 attenuates discrete sub-chronic and early postnatal phencyclidine (PCP)-induced cognitive deficits in rats. *Psychopharmacology (Berl)* **221**:451–468.

Sanacora G and Schatzberg AF (2015) Ketamine: promising path or false prophecy in the development of novel therapeutics for mood disorders? *Neuropsychopharmacology* **40**:259–267.

Sarantis K, Sotiriou E, Papatheodoropoulos C, Matsokis N, and Angelatou F (2008) Differential pharmacological properties of $GABA_A$/benzodiazepine receptor complex in dorsal compared to ventral rat hippocampus. *Neurochem Int* **52**:1019–1029.

Sauguet L, Howard RJ, Malherbe L, Lee US, Corringer PJ, Harris RA, and Delarue M (2013) Structural basis for potentiation by alcohols and anaesthetics in a ligand-gated ion channel. *Nat Commun* **4**:1697.

Saxena RC, Thacore VR, Suri ML, Agarwal TN, and Bhargava KP (1977) Electroencephalographic studies with i.v. methaqualone in man. *Electroencephalogr Clin Neurophysiol* **43**:876–879.

Serafini R, Bracamontes J, and Steinbach JH (2000) Structural domains of the human $GABA_A$ receptor $\beta3$ subunit involved in the actions of pentobarbital. *J Physiol* **524**:649–676.

Sharma V and McNeill JH (2009) To scale or not to scale: the principles of dose extrapolation. *Br J Pharmacol* **157**:907–921.

Sieghart W (2015) Allosteric modulation of $GABA_A$ receptors via multiple drug-binding sites. *Adv Pharmacol* **72**:53–96.

Siegwart R, Jurd R, and Rudolph U (2002) Molecular determinants for the action of general anesthetics at recombinant $\alpha_2\beta_3\gamma_2$ γ-aminobutyric $acid_A$ receptors. *J Neurochem* **80**:140–148.

Sigel E and Lüscher BP (2011) A closer look at the high affinity benzodiazepine binding site on $GABA_A$ receptors. *Curr Top Med Chem* **11**:241–246.

Slany A, Zezula J, Fuchs K, and Sieghart W (1995) Allosteric modulation of [^{3}H]flunitrazepam binding to recombinant $GABA_A$ receptors. *Eur J Pharmacol* **291**:99–105.

Stanley JL, Lincoln RJ, Brown TA, McDonald LM, Dawson GR, and Reynolds DS (2005) The mouse beam walking assay offers improved sensitivity over the mouse rotarod in determining motor coordination deficits induced by benzodiazepines. *J Psychopharmacol* **19**:221–227.

Stewart D, Desai R, Cheng Q, Liu A, and Forman SA (2008) Tryptophan mutations at azi-etomidate photo-incorporation sites on $\alpha1$ or $\beta2$ subunits enhance $GABA_A$ receptor gating and reduce etomidate modulation. *Mol Pharmacol* **74**:1687–1695.

Stewart DS, Hotta M, Li GD, Desai R, Chiara DC, Olsen RW, and Forman SA (2013) Cysteine substitutions define etomidate binding and gating linkages in the α-M1 domain of γ-aminobutyric acid type A ($GABA_A$) receptors. *J Biol Chem* **288**:30373–30386.

Stewart DS, Pierce DW, Hotta M, Stern AT, and Forman SA (2014) Mutations at beta N265 in γ-aminobutyric acid type A receptors alter both binding affinity and efficacy of potent anesthetics. *PLoS ONE* **9**:e111470.

Stórustovu SI and Ebert B (2006) Pharmacological characterization of agonists at δ-containing $GABA_A$ receptors: functional selectivity for extrasynaptic receptors is dependent on the absence of $\gamma2$. *J Pharmacol Exp Ther* **316**:1351–1359.

Thompson SA, Wheat L, Brown NA, Wingrove PB, Pillai GV, Whiting PJ, Adkins C, Woodward CH, Smith AJ, and Simpson PB et al. (2004) Salicylidene salicylhydrazide, a selective inhibitor of $\beta1$-containing $GABA_A$ receptors. *Br J Pharmacol* **142**:97–106.

Trattnig SM, Harpsøe K, Thygesen SB, Rahr LM, Ahring PK, Balle T, and Jensen AA (2012) Discovery of a novel allosteric modulator of 5-HT_3 receptors: inhibition and potentiation of Cys-loop receptor signaling through a conserved transmembrane intersubunit site. *J Biol Chem* **287**:25241–25254.

Wafford KA, Bain CJ, Quirk K, McKernan RM, Wingrove PB, Whiting PJ, and Kemp JA (1994) A novel allosteric modulatory site on the $GABA_A$ receptor β subunit. *Neuron* **12**:775–782.

Wafford KA, van Niel MB, Ma QP, Horridge E, Herd MB, Peden DR, Belelli D, and Lambert JJ (2009) Novel compounds selectively enhance δ subunit containing $GABA_A$ receptors and increase tonic currents in thalamus. *Neuropharmacology* **56**: 182–189.

Walters RJ, Hadley SH, Morris KD, and Amin J (2000) Benzodiazepines act on $GABA_A$ receptors via two distinct and separable mechanisms. *Nat Neurosci* **3**: 1274–1281.

Whiting PJ (2003) GABA-A receptor subtypes in the brain: a paradigm for CNS drug discovery? *Drug Discov Today* **8**:445–450.

Wieland HA, Lüddens H, and Seeburg PH (1992) A single histidine in $GABA_A$ receptors is essential for benzodiazepine agonist binding. *J Biol Chem* **267**: 1426–1429.

Wingrove PB, Wafford KA, Bain C, and Whiting PJ (1994) The modulatory action of loreclezole at the γ-aminobutyric acid type A receptor is determined by a single amino acid in the $\beta2$ and $\beta3$ subunit. *Proc Natl Acad Sci USA* **91**:4569–4573.

Wooltorton JR, Moss SJ, and Smart TG (1997) Pharmacological and physiological characterization of murine homomeric $\beta3$ $GABA_A$ receptors. *Eur J Neurosci* **9**: 2225–2235.

Xue BG, Friend JM, and Gee KW (1996) Loreclezole modulates [^{35}S]t-butylbicyclophosphorothionate and [^{3}H]flunitrazepam binding via a distinct site on the $GABA_A$ receptor complex. *Eur J Pharmacol* **300**:125–130.

Zhong Y and Simmonds MA (1997) Interactions between loreclezole, chlormethiazole and pentobarbitone at $GABA_A$ receptors: functional and binding studies. *Br J Pharmacol* **121**:1392–1396.

Address correspondence to: Anders A. Jensen, Department of Drug Design and Pharmacology, Faculty of Health and Medical Sciences, University of Copenhagen, Denmark. E-mail: aaj@sund.ku.dk